



**HAL**  
open science

# Synthesis and Biological Characterization of Fluorescent Cyclipostins and Cyclophostin Analogues: New Insights for the Diagnosis of Mycobacterial-Related Diseases

Morgane Sarrazin, Benjamin Martin, Romain Avellan, Giri Raj Gnawali, Isabelle Poncin, Hugo Le Guenno, Christopher Spilling, Jean-François Cavalier, Stéphane Canaan

## ► To cite this version:

Morgane Sarrazin, Benjamin Martin, Romain Avellan, Giri Raj Gnawali, Isabelle Poncin, et al.. Synthesis and Biological Characterization of Fluorescent Cyclipostins and Cyclophostin Analogues: New Insights for the Diagnosis of Mycobacterial-Related Diseases. *ACS Infectious Diseases*, 2022, 10.1021/acsinfecdis.2c00448 . hal-03868888

**HAL Id: hal-03868888**

**<https://amu.hal.science/hal-03868888>**

Submitted on 24 Nov 2022

**HAL** is a multi-disciplinary open access archive for the deposit and dissemination of scientific research documents, whether they are published or not. The documents may come from teaching and research institutions in France or abroad, or from public or private research centers.

L'archive ouverte pluridisciplinaire **HAL**, est destinée au dépôt et à la diffusion de documents scientifiques de niveau recherche, publiés ou non, émanant des établissements d'enseignement et de recherche français ou étrangers, des laboratoires publics ou privés.

# **Synthesis and Biological characterization of Fluorescent Cyclopostins & Cyclophostin Analogs: new Insights for the Diagnosis of Mycobacterial-related Diseases**

Morgane Sarrazin,<sup>a,#</sup> Benjamin P. Martin,<sup>b,#</sup> Romain Avellan,<sup>a,#</sup> Giri Raj Gnawali,<sup>b,#</sup> Isabelle Poncin,<sup>a</sup> Hugo Le Guenno,<sup>c</sup> Christopher D. Spilling,<sup>b,\*</sup> Jean-François Cavalier,<sup>a,\*</sup> Stéphane Canaan<sup>a,\*</sup>

<sup>a</sup> Aix-Marseille Univ, CNRS, LISM, IMM FR3479, Marseille, France

<sup>b</sup> Department of Chemistry & Biochemistry, University of Missouri St. Louis, One University Boulevard, St. Louis, MO 63121.

<sup>c</sup> Microscopy Core Facility, IMM FR3479, CNRS, Aix-Marseille Univ, Marseille, France

# These authors should be considered as equal first authors.

\* To whom correspondence should be addressed:

E-mail address: [canaan@imm.cnrs.fr](mailto:canaan@imm.cnrs.fr) (S. Canaan); <https://orcid.org/0000-0001-7478-300X>

E-mail address: [jfcavalier@imm.cnrs.fr](mailto:jfcavalier@imm.cnrs.fr) (J.-F. Cavalier); <https://orcid.org/0000-0003-0864-8314>

E-mail address: [SpillingC@msx.umsl.edu](mailto:SpillingC@msx.umsl.edu) (C.D. Spilling)

## ABSTRACT

Patients with cystic fibrosis (CF) have a significantly higher risk of acquiring nontuberculous mycobacteria infections, predominantly due to *M. abscessus*, than the healthy population. Because *M. abscessus* infections are a major cause of clinical decline and morbidity in CF patients, improving treatment and the detection of this mycobacterium in the context of a polymicrobial culture represents a critical component to better manage patient care. We report here the synthesis of fluorescent Dansyl derivatives of four active Cyclosporins and Cyclosporin analogs (**CyC**) and provide new insights regarding the **CyC** lack of activity against Gram-negative and Gram-positive bacteria, and above all into their mode of action against intramacrophagic *M. abscessus* cells. Our results pointed out that the intracellularly active **CyC** accumulate in acidic compartments within macrophage cells; that this accumulation appears to be essential for their delivery to mycobacteria-containing phagosomes, and consequently, for their antimicrobial effect against intracellular replicating *M. abscessus*; and that modification of such intracellular localization *via* disruption of endolysosomal pH strongly affect the **CyC** accumulation and efficacy. Moreover, we discovered that these fluorescent compounds could become efficient probes to specifically label mycobacterial species with high sensitivity, including *M. abscessus* in presence several other pathogens like *P. aeruginosa* and *S. aureus*. Collectively, all present and previous data emphasized the therapeutic potential of unlabeled **CyC**, and the attractiveness of the fluorescent **CyC** as potential new efficient diagnostic tool to be exploited in future diagnostic developments against mycobacterial-related infections, especially against *M. abscessus*.

## KEYWORDS

Drug susceptibility; Fluorescence microscopy; *M. abscessus*; Probes

Pulmonary diseases caused by mycobacterial species still continues to result in significant morbidity and mortality to human health. In addition to *Mycobacterium tuberculosis* the etiologic agent of tuberculosis (TB),<sup>1</sup> non-tuberculous mycobacteria (NTM) are opportunistic pathogens responsible for a wide spectrum of clinical syndromes, ranging from skin infections (*i.e.*, *Mycobacterium ulcerans* and *Mycobacterium marinum*<sup>2</sup>) to pulmonary infections (*Mycobacterium avium* and *Mycobacterium abscessus* complexes) in humans with compromised natural defenses.<sup>3-4</sup> Although the NTM group comprises more than 200 different species,<sup>5</sup> *M. avium* and *M. abscessus* complexes are the most frequently encountered pathogenic species. They are associated with pulmonary diseases, accounting for >90% of all reported cases of NTM-pulmonary infection.<sup>6-7</sup> *M. abscessus* causes TB-like pulmonary diseases in immunocompromised<sup>8</sup> and vulnerable individuals, including cystic fibrosis (CF) and bronchiectasis patients.<sup>9-11</sup> *M. abscessus* exists as two distinct colony morphotypes, smooth (S) and rough (R), which may evolve differently in response to host immunity, resulting in different fates for the mycobacteria in its host.<sup>12-14</sup> The R variant is often associated with severe pulmonary infections<sup>15-16</sup> and is likely to persist for years, especially in infected CF patients.<sup>17</sup> Moreover, lung infection of CF patients is usually polybacterial<sup>18-19</sup> including combinations of Gram-negative (*i.e.*, *Pseudomonas aeruginosa*, *Haemophilus influenzae* and *Burkholderia cepacia* complex) and Gram-positive bacteria (*i.e.*, *Staphylococcus aureus*), as well as NTM species where *M. abscessus* represents up to 68% of all isolated NTM.<sup>9, 20-21</sup> Furthermore, the fact that this mycobacterium is one of the most drug-resistant mycobacterial species, often referred to as an “antibiotic nightmare”,<sup>22</sup> its presence prior to lung transplantation is a major risk factor for developing a pulmonary infection or a disseminated disease post-surgery.<sup>23</sup> Therefore, there is an emergency to discover new efficient antibiotics and in the context of polybacterial infection involving mycobacteria, it is of utmost importance to discriminate between the various species, and in particular to quickly detect the presence of *M. abscessus* to rapidly determine a specific therapeutic course.

To reach this objective, the Cyclopiostins and Cyclophostin analogs (namely the **CyCs** – **Figure 1**) represent useful and powerful tools.<sup>24</sup> Indeed, a series of 38 monocyclic enol-phosphate (X=O,

**Figure 1A**) and -phosphonate (X=CH<sub>2</sub>, CF<sub>2</sub>, **Figure 1A**) derivatives have been found to efficiently inhibit the growth of *M. tuberculosis* both *in vitro* as well as in infected macrophages with very low toxicity towards the host cells.<sup>25</sup> Furthermore, susceptibility testing conducted on various mycobacterial clinical isolates and bacteria responsible for nosocomial infections; including 6 Gram-negative and 5 Gram-positive bacteria, 29 rapid-growing mycobacteria belonging to the *M. chelonae-abscessus* clade and 2 slow-growing mycobacteria (*M. marinum*, *M. bovis* BCG); revealed that some **CyCs** exhibited very promising minimal inhibitory concentrations (MIC) values, but also that their antibacterial activity was exclusively restricted to mycobacteria.<sup>26</sup> Notably, the enolphosphate **CyC17** was found as the most potent extracellular inhibitor (**Figure 1**) with MICs comparable to those of most classical antibiotics used to treat either *M. tuberculosis* or *M. abscessus* infections.<sup>25-26</sup> Interestingly, its phosphonate analog (*i.e.*, **CyC11**) was inactive against the latter two mycobacteria with MIC > 100 μM.<sup>25, 27</sup> Moreover, among all tested **CyC** analogs, only **CyC7(α,β)** and **CyC8(α,β)** (**Figure 1**) were able to impair intracellular replication of *M. tuberculosis*<sup>25</sup> and *M. abscessus*<sup>27</sup> inside Raw264.7 macrophages, with MIC<sub>50Raw</sub> values better than those of the reference antibiotics rifampicin and imipenem, respectively.

Since these inhibitors act *via* the formation of a covalent bond between the enol-phosphorous atom and the catalytic Ser or Cys residue,<sup>26, 28-30</sup> by using activity-based protein profiling (ABPP), the target enzymes impacted by the **CyCs** were next identified, demonstrating that these compounds are multi-target inhibitors. Indeed, the **CyCs** impair various mycobacterial (Ser/Cys)-base enzymes mostly involved in the whole bacterial lipid metabolism or cell-wall synthesis processes.<sup>27</sup>

Collectively, all these results emphasized the attractiveness of the **CyCs**, that are non-toxic towards mammalian cells and specific to mycobacteria, to be exploited in future therapeutic developments against mycobacterial-related infections, especially against *M. abscessus*.<sup>26</sup>

In this context, the modification of the **CyC** core-structure by the direct introduction of a fluorescent moiety (**Figure 1**) could result in an activity-based probe (ABP), as a means to specifically label living mycobacterial species through the covalent binding to (Ser/Cys)-based enzymes. Such a

fluorescent **CyC**-ABP would also help monitoring and quantifying the **CyC** penetration inside the bacterial cells based on the fluorescent signal.<sup>31-32</sup>

By synthesizing several selected fluorescent **CyC** that displayed potent antibacterial activity against either extracellular or intracellular replicating mycobacteria, we not only evaluated their penetration properties, but above all developed a new, powerful and efficient diagnostic tool to specifically identified *M. abscessus* in a polybacterial mixture to help in the treatment of diseases related to mycobacterial infection.

## RESULTS

**Synthesis of new fluorescent CyC affinity probes.** The **CyC<sub>7α</sub>** and **CyC<sub>7β</sub>** active against intramacrophagic mycobacteria, and the **CyC<sub>17</sub>** active against extracellular replicating mycobacteria as well as its inactive phosphonate counterpart **CyC<sub>11</sub>**, were chosen for incorporation of a fluorescent tag. Moreover, with regards to the mechanism of action of these three **CyCs** towards Ser-/Cys-based enzymes,<sup>26, 28-30</sup> the fluorophore would be placed either on the terminal R<sup>2</sup> chain at the C-5 carbon atom for the *cis* and *trans* isomers of **CyC<sub>7</sub>** (n=6, **Figure 1C**); or on the phosph(on)ate ester moiety for the **CyC<sub>17</sub>** and **CyC<sub>11</sub>** (n=13, **Figure 1C**) by adaption of the chemistry already developed for the synthesis of such derivatives.<sup>25, 27, 33-35</sup> Based upon its spectral properties such as a large Stokes shift, its wide usage in such areas as pharmacology, toxicology, organic synthesis and biochemistry,<sup>36-37</sup> and because it is the smallest available fluorophore, the Dansyl group was chosen as a fluorescent probe.

*Introduction of a Fluorescent group at the C-5 carbon atom.* The initial approach to introduce a label at C-5 employed late stage installation of the fluorescent group *via* coupling to a primary amine, an approach biologically compatible with fluorescent Dansyl molecule. This chemical route (**Figure S1**) involved the application of the phthalimide protecting group at the terminal alkyl chain on the C-5 of the enolphosphonate **9**, which after removal would react with Dansyl-chloride therefore giving the

desire **CyC<sub>7</sub>-Dansyl** derivative. However, despite all our efforts, the desire molecule was only obtained in very low overall 4% yields.

Given the difficulties experienced with the late stage introduction of the fluorescent label, an alternative approach was devised in which the fluorescent tag is introduced earlier in the synthesis. The amine **2** was first reacted with Dansyl-chloride under stirring at room temperature in CH<sub>2</sub>Cl<sub>2</sub>, giving alkenyl sulfonamide **11** in 81% yields. Further coupling reaction with phosphonate **4** *via* cross-metathesis using Grubb's second-generation catalyst afforded carbonate **12** in 90% yields. Then the fluorescent monocyclic enolphosphonate **CyC<sub>7</sub>( $\alpha,\beta$ )-Dansyl** was obtained in racemic form following classical route (**Figure 2A**): *i*) palladium(0)-catalyzed reaction of carbonate **12** with methyl acetoacetate, *ii*) reduction with hydrogen over palladium on carbon in methanol, and *iii*) selective mono-demethylation with sodium iodide followed by cyclization with HBTU.

As previously demonstrated in the synthesis of racemic bicyclic phosphonate analogs,<sup>28</sup> **CyC<sub>7</sub>** compound was characterized by the relationship between the OMe on phosphorus and the H-substituent on the C-5 carbon atom as being either in a *trans* ( $\alpha$ -isomer) or *cis* ( $\beta$ -isomer) relationship (**Figure 1B**). Accordingly, the two racemic diastereoisomers **CyC<sub>7</sub> $\alpha$ -Dansyl** and **CyC<sub>7</sub> $\beta$ -Dansyl** were further separated by careful silica gel column chromatography.

*Introduction of a Fluorescent label at Phosphorus.* In order to introduce the Dansyl group on the alkyl chain at the phosphorus atom, we first examined the use of cross metathesis to build the required functionalized alkane chain with **CyC<sub>11</sub>**, the phosphonate analog of **CyC<sub>17</sub>**. Two alternative routes were used (**Figure S2**). The first one involved metathesis of 6-bromohex-1-ene and Dansyl-amide alkene **11** using Grubb's second-generation catalyst, followed by coupling reaction of resulting alkyl bromide **15** with **CyC<sub>4</sub>**,<sup>24,33</sup> and finally, hydrogenation of the resulting phosphonate ester **16** (**Figure S2A**). Alternatively, the **CyC<sub>11</sub>-Dansyl** was obtained by transesterification of **CyC<sub>4</sub>** with 6-bromo-1-hexene, followed by cross metathesis reaction with the Dansyl-amide alkene **11** and subsequent hydrogenation (**Figure S2B**). In both cases, HRMS data and LC-MS spectra showed the presence of a mixture of compounds with various chain lengths (*i.e.*, M-CH<sub>2</sub>, M and M+CH<sub>2</sub> – **Figure S2C-D**).

Similar variation of ring size from ring closing metathesis reaction had previously been observed in the total synthesis of Dolabelide C.<sup>38</sup> These later byproducts were presumed to occur from double bond isomerization followed by ring-closing metathesis, and resulting there in smaller macrocycles. Here, the chain length variation may also result from the isomerization of the terminal double bond during the cross metathesis (**Figure S2C**).

To overcome such product heterogeneity, two new Dansyl-labeled CyCs were synthesized starting from commercially available 11-Bromo-1-undecanol **18** (**Figure 2B**). The enolphosphonate CyC<sub>31</sub> analogue of CyC<sub>17</sub>, and its phosphate derivative CyC<sub>32</sub> analogue of CyC<sub>11</sub>, were then obtained with a shorter C<sub>11</sub>H<sub>23</sub> alkyl chain on the phosphorus atom *versus* a C<sub>16</sub>H<sub>33</sub> chain for the CyC<sub>17</sub> and CyC<sub>11</sub>. Briefly, following a published procedure,<sup>39</sup> compound **18** was first converted to the 11-amino-1-undecanol **19**<sup>40</sup> in a Gabriel synthesis employing the Ing-Mansk<sup>41</sup> variation. Treatment with boiling HBr<sup>42</sup> converted the alcohol group of **19** to the bromine **20**, which was reacted with Dansyl-chloride to give the Dansyl-labeled bromide compound **21** in 55% yields. Ester exchange reaction process with either the phosphate CyC<sub>16</sub><sup>24, 35</sup> or the phosphonate CyC<sub>4</sub> in presence of an excess Dansyl-bromide **21** and TBAI in refluxing toluene yielded the corresponding fluorescent labeled alkyl phosphate CyC<sub>31</sub>-Dansyl or phosphonate CyC<sub>32</sub>-Dansyl derivative in 43% yields (**Figure 2B**). In parallel, the respective unlabeled analogs, *i.e.* CyC<sub>31</sub> and CyC<sub>32</sub>, were also synthesized in 38-42% yields using the one-pot ester exchange process from CyC<sub>16</sub> and CyC<sub>4</sub>, respectively, and the commercially 1-bromoundecane (**Figure 2C**).

**The new CyC-Dansyl affinity probes retain antibacterial activity similar to that of their parent molecules.** The antimicrobial potency of the selected CyCs [CyC<sub>7(α,β)</sub>-Dansyl, CyC<sub>31</sub>-Dansyl, CyC<sub>32</sub>-Dansyl, as well as CyC<sub>31</sub> and CyC<sub>32</sub>] was next evaluated towards the non-pathogenic *M. smegmatis* strain, four pathogenic mycobacterial species (*i.e.*, *M. marinum*, *M. bovis* BCG, *M. tuberculosis* mc<sup>2</sup>6230, and both S/R variants of *M. abscessus*), 2 Gram-negative (*i.e.*, *Escherichia coli* and *Pseudomonas aeruginosa*) and 1 Gram-positive (*i.e.*, *Staphylococcus aureus*) bacteria. The

corresponding **CyCs** minimal concentration leading to 90% bacterial growth inhibition (*i.e.*, MIC<sub>90</sub>), as determined by the resazurin microtiter assay (REMA),<sup>25-27</sup> are reported in **Table 1**.

As previously reported with the other **CyCs**<sup>26-27</sup> the *in vitro* growth of *E. coli*, *P. aeruginosa* and *S. aureus* was not impacted. Satisfyingly, the *trans*-( $\alpha$ )- and *cis*-( $\beta$ )-isomers of the **CyC7-Dansyl** retained extracellular activity comparable to the parent unlabeled molecules, with a fold change in MIC<sub>90</sub> ranging from 0.7-3.2  $\mu$ M (**Table 1**). In addition, each respective labeled and unlabeled pair of the new phosphate and phosphonate esters bearing a medium lipophilic C11 alkyl chain at the R<sup>3</sup> position, *i.e.*, **CyC31 / CyC31-Dansyl** and **CyC32 / CyC32-Dansyl** (**Figure 2B-C**), displayed similar antibacterial activity against the five mycobacteria, respectively. Interestingly, **CyC31** and **CyC32** exhibited similar MIC<sub>90</sub> values to **CyC17** against *M. bovis* BCG (MIC<sub>90</sub> = 0.87-1.1 vs. 0.80  $\mu$ M) and *M. tuberculosis* (MIC<sub>90</sub> = 5.3 vs. 2.6  $\mu$ M). Surprisingly, in the case of *M. abscessus*, although the **CyC32 / CyC32-Dansyl** phosphonate analogs were almost inactive, the **CyC31** and **CyC31-Dansyl** phosphate esters displayed very good (MIC<sub>90</sub> = 1.2-6.1  $\mu$ M) to moderate (MIC<sub>90</sub> = 27.1-63.4  $\mu$ M) antimycobacterial activity against the S and R variant, respectively (**Table 1**).

The cytotoxicity of the 6 new **CyCs** was also assessed using murine Raw264.7 macrophages.<sup>43</sup> As expected from previous toxicity results obtained with the **CyC1-30**,<sup>25,27</sup> these new **CyCs** showed again a very low toxicity towards host mammalian cells with CC<sub>50</sub>>100  $\mu$ M (**Table 2**), similarly to AMK (CC<sub>50</sub>  $\geq$ 150  $\mu$ M).<sup>44</sup> Given these results, the ability of the **CyC** analogs to inhibit *M. abscessus* intramacrophagic growth was investigated as reported previously.<sup>27</sup> Murine Raw264.7 macrophage cells were infected with *M. abscessus* S-LuxAB<sup>45</sup> at a multiplicity of infection (MOI) of 10, and then incubated for 24 h with various concentration of each **CyC-Dansyl**, or imipenem (IMP; 267  $\mu$ M; 43 $\times$ MIC<sub>90</sub>) used as positive drug control. First, whatever the concentration used, the **CyC31-Dansyl**, **CyC32-Dansyl** as well as the unlabeled **CyC31** and **CyC32** remained fully inactive towards infected macrophages (**Table 2**). Conversely, and in agreement with previous work,<sup>27</sup> both ( $\alpha$ )- and ( $\beta$ )-isomers of **CyC7-Dansyl**, inactive against extracellular bacilli, displayed a moderate activity against

intracellular *M. abscessus* S with a calculated MIC<sub>50Raw</sub> of 39.9  $\mu$ M and 80.6  $\mu$ M, respectively, similar to that of unlabeled **CyC7 $\alpha$**  and **CyC7 $\beta$**  (**Table 2**).

Overall, these results indicate that incorporation of a fluorescent Dansyl group either at the C5 carbon atom (*i.e.*, **CyC7-Dansyl**) or at the R<sup>3</sup> chain on the phosphorus (*i.e.*, **CyC31-Dansyl** & **CyC32-Dansyl**) does not affect the extracellular or intracellular antibacterial activity of the resulting **CyC-Dansyl** fluorescent affinity-based probes, as compared to the unlabeled parent molecules.

**The CyC-Dansyl analogs label mycobacterial strains whatever their antibacterial activity.** To further investigate whether the fluorescent **CyCs** were able to penetrate into the above-mentioned bacteria, each strain was preincubated with the **CyC-Dansyl**. The obtained **CyC-Dansyl**-treated bacteria were visualized by fluorescence microscopy, and total fluorescence related to the Dansyl group was quantified using a Tecan Spark 10 M multimode microplate reader (**Figure 3** & **Figure S3**).

Surprisingly, each of the four **CyC-Dansyl** were found to penetrate efficiently and label all mycobacterial species tested, regardless of their respective MIC values (**Figure 3A**). In particular, the **CyC7 $\alpha$ -Dansyl** and **CyC7 $\beta$ -Dansyl** almost exclusively active against intracellular bacterial growth, are also able to efficiently tag mycobacteria *in vitro*. Quantification of total fluorescence intensity of the four **CyC-Dansyl** incubated with the mycobacterial strains revealed a similar overall profile (**Figure S3**). However, significant variations in fluorescence level were obtained between each **CyC** (**Figure 3B**). Indeed, the mean fluorescence values of the **CyC7 $\beta$ -Dansyl**-treated *M. smegmatis* (23,000 $\pm$ 8,756 au) and both the **CyC7( $\alpha,\beta$ )-Dansyl**-treated *M. abscessus* S (34,874 $\pm$ 5,363 au) and *M. abscessus* R (18,066 $\pm$ 2,279 au) were found significantly 1.2- to 2.8-fold higher ( $p$ -value $<$ 0.001, **Figure 3B**) than those of the respective **CyC31-Dansyl** and **CyC32-Dansyl**-treated mycobacteria. In contrast, no significant difference was observed with *M. Marinum*, *M. bovis* BCG or *M. tuberculosis* labeled strains whatever the **CyC-Dansyl** used (**Figure 3B**). When **CyC7 $\alpha$ -Dansyl**- (*data not shown*) or **CyC31-Dansyl**-treated *M. abscessus* S cells were subjected to cellular fractionation followed by in-gel fluorescence scanning, the inhibitor was found within both the insoluble (*i.e.*, cell wall/membrane) and soluble (*i.e.*,

cytoplasm) fractions (**Figure 3C** & **Figure S4**). Moreover, 3-D reconstruction of confocal laser scanning microscopy images of **CyC<sub>31</sub>-Dansyl**-treated *M. abscessus* S cells confirmed that the diffuse fluorescence (*i.e.*, green and orange resulting colors) observed with the **CyC-Dansyl**-treated strains would result from a homogeneous distribution of these inhibitors in the cell wall and in the cytoplasm (**Figure 3D** and **Movie S1**). Such observations agree with our all previous works, where identified protein targets of the **CyCs** in *M. abscessus* (**CyC<sub>17</sub>** and **CyC<sub>26</sub>**) and *M. tuberculosis* (**CyC<sub>17</sub>**) were originated from both cellular compartments.<sup>25, 27</sup>

**The CyC-Dansyl analogs are unable to label Gram-positive and Gram-negative bacteria, but can react with their respective lysates.** Conversely and in good agreement with MIC data and previous published work with the **CyC**,<sup>26</sup> no significant fluorescence signal was detected when treating *E. coli*, *P. aeruginosa* or *S. aureus* with the four **CyC-Dansyl** probes (**Figure S5**), thus suggesting that the **CyCs** would not be able to cross the cell wall of these latter bacteria. To check if these inhibitors would however be able to react with bacterial enzymes, a lysate of each of the three above-mentioned bacteria was incubated with each **CyC-Dansyl**, then equal amounts of the obtained labeled proteome were separated by 12% SDS-PAGE and visualized by Coomassie staining or in-gel fluorescence for Dansyl detection using a ChemiDoc MP Imager (Bio-Rad) (**Figure S6**). In each treated lysate, clear distinct fluorescent bands were detected corresponding to bacterial (Ser/Cys)-enzymes that presumably had reacted with the **CyC-Dansyl** probes. Given together, these findings confirm that the absence of antibacterial activity of the **CyCs** clearly result from their inability to cross the cell wall of Gram-positive and Gram-negative bacteria.

In the context of CF patients, the presence of numerous Gram-negative and Gram-positive bacteria from the microbiota represents a significant challenge for detecting mycobacteria in sputum.<sup>46</sup> Therefore, we examined the ability of the **CyC-Dansyl** to specifically label *M. abscessus* in polymicrobial cultures. Exponential cultures of *P. aeruginosa*, *S. aureus* and *M. abscessus* S harboring a tdTomato fluorophore were mixed at a 10:10:1 cell ratio, incubated overnight in a 7H9-S medium for mycobacteria enrichment, and then stained with **CyC<sub>31</sub>-Dansyl** probe. In line with our

results, we observed the selective staining of *M. abscessus* in this mixed microbial culture (**Figure 3E**). To assess the sensitivity of the **CyC<sub>31</sub>-Dansyl**, different ratios of the polymicrobial culture were tested. Imaging results showed that the **CyC<sub>31</sub>-Dansyl** could detect a single mycobacterium in the presence of 1000 other bacteria (**Figure 3E**). Taken together, these results confirm that the **CyC-Dansyl** are highly specific and selective for mycobacteria with high sensitivity.

**The CyC-Dansyl affinity probes efficiently label intramacrophagic *M. abscessus*.** In parallel, we investigated the ability of the **CyC-Dansyl** analogs to interact with *M. abscessus* S-tdTomato within infected Raw264.7 macrophage cells. Raw264.7 macrophages were first incubated with each **CyC-Dansyl** probe at a 100  $\mu$ M final concentration for 24 h, and then processed for fluorescent microscopy (**Figure 4 & Figure S7**). At this stage, and despite a similar hydrophobicity between all **CyC-Dansyl** (*i.e.*, mean Log P =  $4.51 \pm 0.24$ ), two different fluorescence profiles were observed depending on the compounds used (**Figure 4A,C & Figure S7A,C**).

With the **CyC<sub>31</sub>-Dansyl** (**Figure 4A**) and **CyC<sub>32</sub>-Dansyl** (**Figure S7A**) a large and diffuse fluorescence was observed inside the macrophage. Remarkably, and despite the absence of intracellular antibacterial activity, infection of the latter **CyC<sub>31/32</sub>-Dansyl**-treated cells with *M. abscessus* S-tdTomato resulted in a clear re-colocalization of the Dansyl inhibitors with the mycobacteria. Moreover, when the Raw264.7 were infected prior to incubation with **CyC<sub>31/32</sub>-Dansyl**, the same final colocalization was also observed. A quantitative analysis of **CyC<sub>31/32</sub>-Dansyl** accumulation in *M. abscessus* S-tdTomato infected macrophages revealed a higher level of each **CyC-Dansyl** associated with the mycobacteria than the Raw264.7 cells (average mean intensity [au] of  $99.38 \pm 1.32$  vs.  $21.29 \pm 1.10$  and  $156.9 \pm 1.91$  vs.  $25.41 \pm 1.19$  for **CyC<sub>31</sub>-Dansyl** and **CyC<sub>32</sub>-Dansyl** positive bacteria vs. positive Raw264.7 cells, respectively; *p-value* < 0.001) (**Figure 4E & Figure S7E**). Analysis of the distribution of each **CyC-Dansyl** mean intensity between intracellular *M. abscessus* S-tdTomato and Raw264.7 cells areas by density plot confirms that *M. abscessus* bacteria displayed a higher **CyC-Dansyl** signal enrichment than macrophage cells (**Figure 4F & Figure S7F**). These findings are consistent with a dynamic relocation

process of the **CyC** inside the macrophage and leading to a clear tropism of both **CyC<sub>31/32</sub>-Dansyl** for intracellular *M. abscessus* S.

In contrast, when macrophages were treated with the **CyC<sub>7(α,β)</sub>-Dansyl**, which are active mainly in intracellular conditions, a totally different behavior than the other two **CyC<sub>31/32</sub>-Dansyl** compounds was reached (**Figure 4C & Figure S7C**). Indeed, their fluorescence was mainly localized into foci as if these two inhibitors accumulated in specific cell compartments. Interestingly, after infection both **CyC<sub>7(α,β)</sub>-Dansyl** colocalized with the intracellular mycobacteria (**Figure 4C,D & Figure S7C,D**), as also observed with the **CyC<sub>31/32</sub>-Dansyl** inhibitors. In addition, the quantitative analysis of **CyC<sub>7(α,β)</sub>-Dansyl** accumulation in *M. abscessus* S-tdTomato infected macrophages revealed a higher level of each **CyC<sub>7</sub>-Dansyl** associated with the mycobacteria than the Raw264.7 cells (average mean intensity [au] of  $144.6 \pm 2.25$  vs.  $31.85 \pm 2.34$ , and  $137.2 \pm 2.13$  vs.  $48.78 \pm 2.25$  for **CyC<sub>7α</sub>-Dansyl** and **CyC<sub>7β</sub>-Dansyl** positive bacteria vs. positive Raw264.7 cells, respectively; *p*-value < 0.001) (**Figure 4E & Figure S7E**). Such tropism was further confirmed by analysis of the distribution of **CyC<sub>7(α,β)</sub>-Dansyl** fluorescence intensity between intracellular *M. abscessus* S-tdTomato and Raw264.7 cells by density plot (**Figure 4G & Figure S7G**).

**The **CyC<sub>7(α,β)</sub>-Dansyl** analogs accumulate in acidic intracellular compartments.** Among the four **CyC-Dansyl** analogs tested, the fact that only the **CyC<sub>7(α,β)</sub>-Dansyl** are active against intramacrophagic replicating bacteria (**Table 2**) prompted us to investigate further their particular localization as foci-like inside macrophages. More precisely, the fact that lysosomes are acidic and hydrolytic organelles responsible for the degradation of macro and small molecules inside macrophages,<sup>47</sup> we tested whether these two compounds accumulate in acidic compartments. Raw264.7 macrophages were then treated with 100 μM of each of the four **CyC-Dansyl** compounds, and acidic compartments were labeled using BioTracker™ NIR633, a deep red-fluorescent dye that labels acidic organelles in live cells. First, in agreement with our previous observation (**Figure 4 & Figure S7**), the **CyC<sub>31</sub>-Dansyl** and **CyC<sub>32</sub>-Dansyl** exhibited a diffuse fluorescence and only few colocalization between the Dansyl and the BioTracker signals were observed inside Raw264.7 cells (**Figure S8**). Conversely, the **CyC<sub>7(α,β)</sub>-Dansyl**

displayed a clear colocalization with BioTracker positive regions (**Figure 5A,B**). Quantitative analysis of the Dansyl fluorescence signal in these BioTracker positive regions showed a significant 1.5 to 1.8-fold change in the average mean intensity for **CyC7 $\alpha$ -Dansyl** ( $85.5\pm 0.76$  au) and **CyC7 $\beta$ -Dansyl** ( $79.8\pm 0.89$  au) vs. **CyC31-Dansyl** ( $48.2\pm 0.85$  au) and **CyC32-Dansyl** ( $51.8\pm 0.89$  au) (**Figure S9**), therefore confirming the preferential colocalization of the **CyC7( $\alpha,\beta$ )-Dansyl** within acidic compartments.

From these findings, **CyC7-Dansyl**-treated macrophages were next incubated in presence of the vacuolar-type H<sup>+</sup>-ATPase inhibitor Concanamycin A (ConA) (*i.e.*, an inhibitor of endolysosomal acidification).<sup>48</sup> Indeed, ConA inhibited endolysosomal acidification resulting in the loss of BioTracker staining, but unexpectedly also impaired the **CyC7-Dansyl** accumulation phenotype resulting in a diffuse Dansyl fluorescence all around the cell, similar to those reached with both **CyC31/32-Dansyl** (**Figure 5A,B & Figure S8A,B**). Furthermore, with infected macrophages the presence of ConA results mainly in the loss of the strict colocalization of the **CyC-Dansyl** with the intracellular mycobacteria (**Figure 5C & Figure S8C**), as observed above in **Figure 4 & Figure S7**. Finally, intracellular antibiotic activity assays performed with 100 nM ConA, led to a complete abrogation of the **CyC7( $\alpha,\beta$ )** inhibitory effects, without altering intramacrophage *M. abscessus* growth or intracellular efficacy of imipenem used as drug control (**Figure 5D**). Since the intracellular activity of the compounds appears to be correlated with acidic compartments, we investigated whether low pH was needed for activating the **CyC** in extracellular conditions. Then, we conducted susceptibility testing at various pH in the 5.5-7.0 range, and showed that **CyC7( $\alpha,\beta$ )** or **CyC31** MIC values against extracellular *M. abscessus* S growth were not modified, thus suggesting that the antibacterial activity of these compounds is not pH-dependent (**Figure 5E**).

## DISCUSSION

The continuous and rapid emergence of drug-resistant mycobacteria, associated with the lack of new antibiotics entering the market, has become a global public health concern that threatens the effective diagnosis and treatment of pulmonary infectious diseases. Infections caused by nontuberculous

mycobacteria (NTM) have now become clinically relevant and are extremely difficult to treat due to the intrinsic resistance of such mycobacteria to many common antibiotics. Among NTM, *M. abscessus* is the most antibiotic-resistant mycobacterial species responsible for severe respiratory, skin and mucosal infections in humans, frequently found in immunocompromised patients or patients with Cystic fibrosis (CF) or chronic obstructive pulmonary disease (COPD).<sup>49-50</sup> In the case of CF patients, *M. abscessus* infection may also be exacerbated by poly-bacterial lung infections with other microorganisms, such as *P. aeruginosa* and/or *S. aureus*.<sup>46</sup> In this context of co-infection, *M. abscessus* would be missed in the absence of effective microbiological surveillance; whereas it is of great importance to accurately detect its presence in patient's sputum in order to adapt the antimicrobial treatment.<sup>22, 49</sup>

Toward the generation of new antibacterial leads, the **CyC** analogs are not only non-toxic for mammalian cells, but above all represent a novel class of selective and efficient multitarget inhibitors leading to the arrest of *M. abscessus* extracellular and/or intracellular growth through the inhibition of various mycobacterial enzymes involved in important physiological processes.<sup>24</sup> Herein, we report an optimized and efficient total synthesis of fluorescent Dansyl derivatives of four active **CyC** analogs, and their use as efficient probes. We demonstrated that these fluorescent **CyC-Dansyl** not only behave similarly to their parent molecules in terms of antibacterial activity and toxicity towards host cells, but also specifically label all mycobacterial species tested, including *M. abscessus* in the context of a poly-bacterial mixture with *P. aeruginosa* and *S. aureus*, with high sensitivity since a single mycobacterium in the presence of  $10^3$  other bacteria can be detected. Moreover, we provide compelling evidence that the absence of antibacterial effect on Gram-positive and Gram-negative bacteria results from the inability of these **CyCs** to cross the bacterial membrane of the latter microorganisms. The most likely hypothesis is that the hydrophobic nature of the **CyCs** would favor their diffusion across the waxy and lipid-rich mycobacterial membrane, unlike that of Gram-positive and Gram-negative bacteria. Such property could be used to the rapid detection of *M. abscessus* in patient's sputum thus paving the way for new promising applications of the **CyCs** in diagnostics.

Another important issue resides in the fact that the penetration of the fluorescent **CyC** inside the mycobacteria was not correlated with their respective MIC values (**Table 1 & Figure 3**). Accordingly, **CyC<sub>32</sub>-Dansyl** and **CyC<sub>7(α,β)</sub>-Dansyl** which are ineffective against *M. abscessus* extracellular growth behave similarly to **CyC<sub>31</sub>-Dansyl** in terms of bacterial fluorescence labeling (**Figure 3B**). This unexpected feature implies that the antibacterial activity of the **CyC** against the extracellular growth of *M. abscessus* would result from the inhibition of mycobacterial target enzymes specific to each compound, as recently demonstrated in the case of *M. tuberculosis*,<sup>51</sup> independently of their penetration properties since they are all capable to enter the mycobacteria. In other words, the discrepancy in terms of extracellular activity between the four **CyC** might simply rely on relative chemical reactivity between the phosphate (*i.e.*, potent **CyC<sub>17</sub>** & **CyC<sub>31</sub>**) and phosphonate (*i.e.*, inactive **CyC<sub>7(α,β)</sub>** & **CyC<sub>32</sub>**) chemical groups.

When tested against *M. abscessus* infected macrophages, each **CyC-Dansyl** probe also perfectly colocalized with intracellular bacterial cells, regardless of their respective intracellular MIC<sub>Raw</sub> values (**Table 2**). A distinct fluorescent profile inside Raw264.7 macrophages was however obtained, depending on the compounds. Following BioTracker labeling, our results clearly suggest that the **CyC<sub>7(α,β)</sub>-Dansyl**, only active against intramacrophagic *M. abscessus* growth, would accumulate preferentially in acidic compartments contrary to **CyC<sub>31/32</sub>-Dansyl** for which a predominantly diffuse fluorescence was observed within the cells (**Figure 5 & Figure S8**). The inhibitor of the vacuolar-type H<sup>+</sup>-ATPase Concanamycin A (ConA) disrupted the intracellular accumulation phenotype of **CyC<sub>7(α,β)</sub>-Dansyl**, drastically abolish their colocalization with intracellular *M. abscessus* inside infected macrophages, and impaired their antibacterial efficacy as shown by intracellular antibiotic susceptibility assays (**Figure 4-5**). Conversely, the presence of ConA did not significantly alter **CyC<sub>31/32</sub>-Dansyl** fluorescent profile inside Raw264.7 cells. These novel results support the idea that in conditions where acidification is suppressed, the ability of the **CyC<sub>7(α,β)</sub>** to accumulate in specific acidic compartments and restrict intramacrophagic *M. abscessus* replication would be limited.

Moreover, the fact that the extracellular antibacterial activity of the **CyC** is not pH-dependent (**Figure 5E**), also presumes that the partitioning and accumulation of **CyC**<sub>7(α,β)</sub> in acidic compartments represents the crucial step that drives their delivery to the mycobacterial containing phagosomes. In a similar way to bedaquiline which accumulates in host lipid bodies (LB) and is transferred to *M. tuberculosis* as LB are consumed thus leading to enhanced antibacterial activity,<sup>52</sup> host cell acidic compartments constitute a transferable reservoir responsible for the **CyC**<sub>7(α,β)</sub> antimicrobial efficacy against intracellularly replicating *M. abscessus*. Consequently, even though endolysosomal acidification appears to be an important determinant contributing to the **CyC**<sub>7(α,β)</sub> intracellular efficacy, their mode of action would differ drastically from that of pyrazinamide<sup>53</sup> or clofazimine<sup>54</sup> for which the pH is the critical issue for the activation of the drug against *M. tuberculosis* infected macrophages. Given all these findings, it is also tempting to hypothesize that the mostly diffuse localization of **CyC**<sub>31/32</sub> inside the cells may be responsible for the lack of intracellular activity.

## CONCLUSION

Diseases caused by pathogenic mycobacterial species continue to cause significant morbidity and mortality to human health. In this context, the discovery few years ago of a very promising family of multi-targeted inhibitors, called Cyclipostins & Cyclophostin analogs (**CyCs**), with potent antimycobacterial activities has opened the way to new therapeutic strategies in the fight against mycobacterial-related diseases. These include *M. tuberculosis* and *M. abscessus*, two major human pathogens responsible for severe lung infections. Moreover, these **CyCs** do not alter the growth of Gram-positive and Gram-negative bacteria and do not exhibit significant toxicity towards mammalian cells. In this work, using several selected fluorescent **CyCs**, we brought new insights into their mode of action against both extracellular and intracellular mycobacterial growth. All this study has not only reinforced the great interest of the **CyC** compounds, but above all our results provide a first set of explanations related to the antibacterial activity of the **CyC**, both *in vitro* and *ex vivo*, underlining the huge and combined effect of the host-cell environment with antibiotics during mycobacterial

infection, and particularly here in the case of *M. abscessus* infections. Apart from the therapeutic potential of unlabeled CyC compounds, thanks to their multitargeted covalent mechanism of action, fluorescent CyC probes could be used to specifically label pathogenic mycobacteria in polybacterial mixtures thus leading to new efficient, selective and sensitive diagnostic markers. This is of particular importance to patients with cystic fibrosis for whom identification of *M. abscessus* is crucial, especially for transplantation purposes.<sup>23</sup>

## METHODS

**Chemistry.** Detailed procedures and the full chemical characterization ( $^1\text{H}$ ,  $^{13}\text{C}$  and  $^{31}\text{P}$  NMR spectra) of each new analog (*i.e.*, the four **CyC-Dansyl** and **CyC<sub>31/32</sub>**) are reported in **Supporting Information**. Stock solutions (10 mM) in which the **CyC** compounds (purity of  $\geq 95\%$ ) were found to be completely soluble in dimethyl sulfoxide (DMSO) were prepared and stored at 4 °C.

**Bacterial culture.** *Escherichia coli* DH10B, *Pseudomonas aeruginosa* PAO1 and *Staphylococcus aureus* (clinical isolate) cells were grown in Luria-Bertani (LB) broth (Invitrogen, Carlsbad CA, USA) at 37 °C under shaking at 200 rpm. *M. smegmatis* was cultured in Middlebrook 7H9 liquid media (BD Difco) supplemented with 0.05% Tween 80 (Sigma-Aldrich, Saint-Quentin Fallavier, France) and 0.2% glycerol (Euromedex, France) (7H9-S). *M. abscessus* CIP104536<sup>T</sup> with either a smooth (S) or a rough (R) morphotype, *M. marinum* ATCC BAA-535/M, *M. bovis* BCG Pasteur 1173P2 and *M. tuberculosis* mc<sup>2</sup>6230 (H37Rv  $\Delta RD1 \Delta panCD^{55}$ ) were cultured in 7H9-S supplemented with 10% Oleic Albumin Dextrose Catalase (OADC enrichment, BD Difco) (7H9-S<sup>OADC</sup>). In the case of *M. tuberculosis* mc<sup>2</sup>6230, 24  $\mu\text{g}/\text{mL}$  D-pantothenate (Sigma-Aldrich) was also added in the 7H9-S<sup>OADC</sup> medium. Recombinant *M. abscessus* S carrying pTEC27 (Addgene, plasmid 30182) expressing red fluorescent tdTomato protein was grown in 7H9-S<sup>OADC</sup> with 500  $\mu\text{g}/\text{mL}$  hygromycin B (Euromedex, France).<sup>56</sup> Recombinant *M. abscessus* S carrying the pSMT3-GFP-LuxAB plasmid allowing luminescence and fluorescence was grown in 7H9-S<sup>OADC</sup> with 1,000  $\mu\text{g}/\text{mL}$  hygromycin B (Euromedex, France).<sup>45</sup> This latter *M. abscessus* S-LuxAB strain was a generous gift from Prof. Jean-Louis Herrmann (Université Versailles-Saint-Quentin-en-Yvelines, France) and was used for measurement of bacterial load inside infected macrophages. All cultures were incubated at 37 °C, except *M. marinum* which was cultured at 32 °C. *M. smegmatis* and *M. abscessus* were stirred at 200 rpm; *M. bovis* BCG, *M. tuberculosis* mc<sup>2</sup>6230 and *M. marinum* at 50 rpm.

**Determination of minimum inhibitory concentrations.** Susceptibility testing for mycobacteria was performed using the Middlebrook 7H9 broth microdilution method. MICs of the **CyCs** were determined in 96-well flat-bottom Nunclon Delta Surface microplates with lid (Thermo-Fisher Scientific, ref. 167008) using the resazurin microtiter assay (REMA) as described previously.<sup>26-27, 57</sup> Briefly, log-phase bacteria were diluted to a cell density of  $5 \times 10^6$  cells/mL in appropriate 7H9-S medium. Then, 100  $\mu$ L of this bacterial suspension ( $5 \times 10^5$  cells per well) was added to each well containing 100  $\mu$ L of the appropriate 7H9-S medium, serial two-fold dilutions of the selected **CyCs** or controls to a final volume of 200  $\mu$ L. Plates were incubated at 37 °C (32 °C for *M. marinum*) for either 3-5 days (*M. smegmatis* and *M. abscessus*) or 7-14 days (*M. marinum*, *M. bovis* BCG and *M. tuberculosis* mc<sup>2</sup>6230). Then, 20  $\mu$ L of 0.025% (w/v) resazurin solution was added and incubation was proceeded for color change (from blue to pink) in the control well (bacteria without antibiotic). Fluorescence of the resazurin metabolite resorufin ( $\lambda_{\text{ex}}/\lambda_{\text{em}} = 530/590 \pm 10$  nm) was quantified using a Tecan Spark 10M multimode microplate reader (Tecan Group Ltd, France). Relative fluorescence units were defined as: RFU% = (test well FU/mean FU of growth control wells)  $\times$  100. MIC values were determined by fitting the RFU% sigmoidal dose-response curves<sup>25, 58</sup> in Kaleidagraph 4.2 software (Synergy Software). The lowest compound concentration leading to 90% bacterial growth inhibition was defined as the MIC<sub>90</sub>.

In parallel, MICs of *E. coli*, *P. aeruginosa* and *S. aureus* were assessed using the broth microdilution method.<sup>59</sup> Log phase bacteria were diluted in LB medium to around  $5 \times 10^5$  cells/mL. Then 100  $\mu$ L of this latter inoculum were added into each well containing serial dilution of the **CyCs**, and the plates were incubated at 37 °C for 18-24 h. After incubation, OD<sub>600nm</sub> was recorded using a Tecan Spark 10M multimode microplate reader (Tecan Group Ltd, France). The MIC was defined as the lowest concentration of **CyC** that inhibited visible growth of the bacteria.

Each assay for each strain was carried out at least in triplicate.

**Determination of Cytotoxic Activity for new CyCs.** The cytotoxicity of each new synthesized CyC against eukaryotic cells was measured based on the reduction of resazurin as a value of cellular viability by metabolic activity.<sup>27, 60</sup> Murine (Raw264.7) macrophages (American Type Culture Collection TIB-71) were cultured from a freezer stock in Dulbecco's modified Eagle medium (DMEM; Gibco) supplemented with 10% heat-inactivated fetal calf serum (FBS, Invitrogen) (DMEM<sup>FBS</sup>). Cells were grown at 37 °C and 5% CO<sub>2</sub> to subconfluent concentrations. Then 5 × 10<sup>4</sup> cells/well were seeded in 96-well flat-bottom Nunclon Delta Surface microplates with lid (ThermoFisher Scientific) in a final volume of 200 μL per well and incubated for additional 24 h. The medium was removed by aspiration, and 200 μL of serial two-fold dilution of each compound (CyC<sub>7(α,β)</sub>-Dansyl, CyC<sub>31</sub>-Dansyl, CyC<sub>32</sub>-Dansyl, as well as CyC<sub>31</sub> and CyC<sub>32</sub>) in DMEM<sup>FBS</sup> were then added to each well. After 24 h incubation, 20 μL of a 0.025% (w/v) resazurin solution was added to each well. Fluorescence was measured following a 4 h incubation at 37 °C and 5% CO<sub>2</sub> in the dark, by excitation at 530 nm and emission at 590 nm as described above, leading to relative metabolic activities. Addition of DMSO was used as 100% viability reference and addition of 0.2% Triton X-100 solution served as negative standard (0% viability). All experiments were performed as two independent triplicates.

**Intramacrophage killing assay.** Raw264.7 macrophages were grown in DMEM<sup>FBS</sup> medium at 37 °C and 5% CO<sub>2</sub> to subconfluent concentrations. Then 5 × 10<sup>4</sup> cells/well were seeded in 96-well flat-bottom Nunclon Delta Surface microplates with lid in a final volume of 200 μL per well and cultured for additional 24 h. The cells were infected with *M. abscessus* S-LuxAB at a multiplicity of infection (MOI) of 1:10 and incubated at 37 °C in the presence of 5% CO<sub>2</sub> for 3 h. Cells were then washed three times with DMEM then refed with DMEM<sup>FBS</sup> supplemented with 200 μg/mL amikacin for 1 h. at 37°C and 5% CO<sub>2</sub> to kill any extracellular bacteria; washed again three times with DMEM prior to the addition of 2-fold dilutions of the CyC compounds or imipenem (IMP) in DMEM<sup>FBS</sup> supplemented with 50 μg/mL (*i.e.*, 85.4 μM) amikacin (200 μL final volume). In each plate, negative

controls consisting of amikacin (50 µg/mL) and 1% DMSO (*i.e.*, infected macrophages only); as well as positive controls containing amikacin (50 µg/mL) plus 80 µg/mL (*i.e.*, 267 µM) IMP were also included.<sup>27, 61</sup> Plates were incubated for 24 h at 37°C, 5% CO<sub>2</sub>.

Luminescence measurement was then used to check intracellular bacterial viability of *M. abscessus* S-LuxAB<sup>45</sup> following treatment with each CyC compound concentration. Infected macrophage cells were first washed three times with PBS and lysed by addition of 200 µL cold PBS-0.1% Triton X-100. A solution of 1% *n*-decanal (Sigma-Aldrich) in ethanol (20 µL) was added in each well after lysis of macrophages, and luminescence was read immediately using a Tecan Spark 10M multimode microplate reader (Tecan Group Ltd, France). DMSO-treated infected macrophages corresponded as control representing 100% of bacterial viability. The luminescence value obtained was next correlated to CFU using a calibration curve  $\text{Log}_{10}(\text{Lux}) = f(\text{Log}_{10}(\text{CFU}))$  initially built by plating 10-fold serial dilutions of *M. abscessus* S-LuxAB on 7H9 agar medium, followed by colonies enumeration after 4-5 days of incubation at 37 °C. Intracellular MIC<sub>Raw</sub> values were further determined by fitting the CFU% sigmoidal dose-response curves in Kaleidagraph 4.2 software (Synergy Software). The lowest compound concentration inhibiting 50% of intracellular bacterial growth was defined as the MIC<sub>50Raw</sub>. Each experiment was done three times independently.

**Mycobacteria and infected/non-infected macrophages labeling with the CyC-Dansyl.** Mid-log phase mycobacterial suspension in appropriate 7H9-S medium was harvested for 15 min at 3,500 rpm, and resuspended in PBS buffer (pH 7.4) containing 0.05% (*v/v*) Tween 20 (Euromedex, France) (PBS-T) at an OD<sub>600</sub> corresponding to  $1.5 \times 10^{10}$  cells/mL. Then, the cells were incubated with 200 µM of each CyC-Dansyl (*i.e.*, CyC<sub>31</sub>-Dansyl, CyC<sub>32</sub>-Dansyl, CyC<sub>7α</sub>-Dansyl and CyC<sub>7β</sub>-Dansyl) or DMSO (negative control) for 3 h at 37 °C (32 °C for *M. marinum*) under shaking at 200 rpm. After incubation, bacteria were washed three times with PBS-T and resuspended in 100 µL PBS-T. For quantification of total fluorescence, 100 µL of each sample (*i.e.*,  $7.5 \times 10^9$  cells/mL) in PBS-T was dispensed in a 96-well Chimney black microplate (Greiner Bio-one, Germany). The fluorescence

related to the Dansyl group was recorded at  $\lambda_{\text{ex}}/\lambda_{\text{em}} = 400/535 \pm 10$  nm using a Tecan Spark 10M multimode microplate reader (Tecan Group Ltd, France). For microscopy observation, the bacteria were fixed with 4% paraformaldehyde in PBS for 1 h at room temperature, washed three times with PBS-T and resuspended in 100  $\mu\text{L}$  PBS-T. Microscopy observations also performed in PBS buffer but in absence of Tween 20, resulted in similar labeling results, thus excluding any interference of detergent in the labeling of mycobacteria (*data not shown*).

Raw264.7 macrophages were grown in DMEM<sup>FBS</sup> medium at 37 °C and 5% CO<sub>2</sub> to subconfluent concentration. Then  $2.5 \times 10^5$  cells/well were seeded in 8-well Nunc Lab-Tek II Chamber Slide System, RS glass (ThermoFisher Scientific) in a final volume of 250  $\mu\text{L}$  per well, and cultured for additional 24 h. Cells were washed three times with DMEM, then refed with DMEM<sup>FBS</sup> supplemented with 100  $\mu\text{M}$  fluorescent **CyC-Dansyl** probes and incubated for additional 24 h at 37 °C and 5% CO<sub>2</sub>. Cells were then washed three times with DMEM, and infected with the fluorescent *M. abscessus* S-tdTomato strain at a MOI of 10 and processed as described above (see *Intramacrophage killing assay* section). Alternatively, the cells were first infected with *M. abscessus* S-tdTomato strain prior to a 24 h-incubation period with 100  $\mu\text{M}$  **CyC-Dansyl** probes. After incubation, the infected and non-infected macrophages were washed three times with sterile PBS, fixed using 4% paraformaldehyde for 15 min, then washed twice with PBS and re-filled with 250  $\mu\text{L}$  PBS.

**Fluorescent Microscopy.** Fixed samples (4  $\mu\text{L}$  bacterial suspension, *i.e.*  $3.0 \times 10^7$  cells, spotted between a microscope slide and coverslip; or macrophage cells in Lab-Tek II Chamber Slide System) were analyzed by snapshot fluorescence imaging at room temperature using an Olympus IX81 confocal microscope equipped with a UPlanSApo 100 $\times$  1.40 NA objective and operated with the FV1000 software. Acquisitions were taken using a 2-line Kalman integration. Exposure time was 10  $\mu\text{s}$ /pixel for both laser transmission and fluorescence images with conserved settings (X, Y, Z, HV, Gain and offset). The Dansyl was detected by excitation with a 405 nm laser with 39-50% intensity, and emission was collected using a semitransparent mirror collecting all wavelength under

560 nm. The tdTomato was detected by excitation with a 515 nm laser with 20-40% intensity, and emission was collected using a semitransparent mirror collecting all wavelength over 560 nm. 3D-fluorescence images were acquired on a DeltaVision OMX SR imaging system from GE Healthcare, with an Olympus PlanApo N 60× 1.42 NA and 2 cameras sCMOS. The Dansyl was detected by a 405 nm diode laser (61 mW) at 2%T during 50 ms and with a 435/31 nm emission filter and the Nile Red was detected by a 568 nm diode-pumped solid-state laser (61mW) at 2%T during 100 ms and with a 609/37 nm emission filter. 11 sections of images of 512 × 512 pixels (pixel size of 80 nm) were acquired with a section spacing of 0.125 μm and a sample thickness of 1.25 μm. Images were then deconvoluted with the microscope software “Softworks 7.0.0” and then analyzed with Fiji 1.53f51. With each CyC-Dansyl probe, two biological replicates were made with infected and non-infected macrophages; and for each sample, 8 different images were taken per frame in order to get more than 200 macrophage cells in total. Images were next converted to an 8-bit intensity color range. In all cases, the corresponding control images were taken/checked prior to any fluorescence imaging and quantification.

**Analysis of Dansyl mean fluorescence intensity** (adapted from<sup>53</sup>). A background noise was first calculated by taking the mean fluorescence intensity of 20 different areas free of any cells for each channel (*i.e.*, Dansyl and tdTomato frames, respectively), and was subtracted to each frame. Segmentation and analysis of the images recorded (126.98 × 126.98 μm; 512 × 512 pixels) were performed using the open source program ImageJ/Fiji 1.53f51. Cells segmentation was done by manually detouring the Raw264.7 cells on the laser transmission frame and transforming it into a mask. This Raw-mask was then used to determine the Dansyl mean fluorescence intensity of pixels associated to the macrophage region and corresponding to the inhibitor cellular uptake. For intracellular bacterial segmentation, a manual threshold was first applied to the tdTomato frame to create a binary mask, defining all bacterial regions of interest. This bacterial-mask was used to

measure the Dansyl mean fluorescence intensity of pixels associated to the *M. abscessus* S-tdTomato region and corresponding to the inhibitor bacterial uptake.

**Live fluorescence imaging and BioTracker staining.** For live-cell imaging, infected and non-infected Raw264.7 macrophages  $\pm$  100 nM ConA and  $\pm$  100  $\mu$ M CyC-Dansyl were washed with PBS buffer (pH 7.4) and stained for 30 min with DMEM<sup>FBS</sup> medium containing 1X BioTracker™ NIR633 Lysosome Dye (Sigma Aldrich) at 37 °C and 5% CO<sub>2</sub> following the manufacturer recommendations. Live-cell imaging was further performed by excitation with a 633 nm laser with 10% intensity, and emission was collected using a semitransparent mirror collecting all wavelength over 560 nm as described above. Segmentation and analysis were performed as described above. First, the background was removed from each CyC-Dansyl and BioTracker frames as described previously. To segment BioTracker positive area, a manual threshold was applied to the BioTracker frames in order to create a binary mask, thereby defining all regions of interest. This BioTracker-mask was further used to quantify the Dansyl mean intensity inside BioTracker positive areas which allowed to compare the uptake of each CyC-Dansyl inhibitor in acidic compartments inside the macrophages.

**Movie S1.** Movie was generated using Dragonfly 2022.1 (ORS) using the same data from **Figure 3D**. A 3D reconstruction was first made and then different views (zoom, rotation, orthoslice) have been selected at different key frame to make the movie.

**Statistical analyses.** Statistical analyses were performed using Prism 4.0 (Graphpad, Inc) and are detailed in each figure legend. Density plot of the resulting fluorescence data was calculated using the distplot tool from the seaborn statistical data visualization python library,<sup>62</sup> and the sinaplot-boxplots were generated with the PlotOfData web tool.<sup>63</sup>

## ASSOCIATED CONTENT

### \* Supporting Information

Supporting Information for this article is available online

Detailed protocols, full chemical characterization, NMR spectra of the new fluorescent **CyC** compounds; **Figures S1-S2**, synthesis of racemic **CyC<sub>7</sub>-Dansyl** and **CyC<sub>11</sub>-Dansyl**; **Figure S3**, fluorescence intensity profile of each **CyC-Dansyl**-treated mycobacteria; **Figure S4**, in gel fluorescence of DMSO-treated total lysate of *M. abscessus*; **Figures S5**, fluorescence intensity profile of **CyC-Dansyl**-treated *E. coli*, *P. aeruginosa* or *S. aureus* bacteria; **Figure S6**, in gel fluorescence of **CyC-Dansyl**-treated total lysate of *E. coli*, *P. aeruginosa* or *S. aureus*; **Figures S7-S9**, fluorescence imaging and quantification of the **CyC-Dansyl** inside infected and non-infected macrophages (PDF).

**Movie S1**, 3-D reconstruction of a stack of deconvoluted images of **CyC<sub>31</sub>-Dansyl**-treated *M. abscessus* S cells from an epi-fluorescence microscope (AVI).

## AUTHOR INFORMATION

### Corresponding Authors

**Christopher D. Spilling** - Department of Chemistry & Biochemistry, University of Missouri St. Louis, One University Boulevard, St. Louis, MO 63121. Email: [SpillingC@msx.umsl.edu](mailto:SpillingC@msx.umsl.edu)

**Jean-François Cavalier** - Aix-Marseille Univ, CNRS, LISM, IMM FR3479, Marseille, France. Email: [jfcavalier@imm.cnrs.fr](mailto:jfcavalier@imm.cnrs.fr). ORCID: <https://orcid.org/0000-0003-0864-8314>

**Stéphane Canaan** - Aix-Marseille Univ, CNRS, LISM, IMM FR3479, Marseille, France. Email: [canaan@imm.cnrs.fr](mailto:canaan@imm.cnrs.fr). ORCID: <https://orcid.org/0000-0001-7478-300X>

### Authors

**Morgane Sarrazin** - Aix-Marseille Univ, CNRS, LISM, IMM FR3479, Marseille, France.

**Benjamin P. Martin** - Department of Chemistry & Biochemistry, University of Missouri St. Louis, One University Boulevard, St. Louis, MO 63121.

**Romain Avellan** - Aix-Marseille Univ, CNRS, LISM, IMM FR3479, Marseille, France.

**Giri Raj Gnawali** - Department of Chemistry & Biochemistry, University of Missouri St. Louis, One University Boulevard, St. Louis, MO 63121.

**Isabelle Poncin** - Aix-Marseille Univ, CNRS, LISM, IMM FR3479, Marseille, France.

**Hugo Le Guenno** - Microscopy Core Facility, IMM FR3479, CNRS, Aix-Marseille Univ, Marseille, France.

## **Author Contributions**

Conceptualization: CDS, SC and JFC. Resources: BPM, GRG and CDS. Investigations: MS, RA, IP and HLG. Formal analysis: MS, RA, HLG, SC and JFC. Funding acquisition: SC and JFC. Supervision: CDS, SC and JFC. Writing-original draft: MS, RA and JFC. Writing-review & editing: MS, RA, HLG, CDS, SC and JFC. MS, BPM, RA and GRG contributed equally and should be considered as first coauthors. All authors have given approval to the final version of the manuscript.

## **Notes**

The authors declare no conflict of interest.

## **ACKNOWLEDGMENTS**

This work was supported by the Centre National de la Recherche Scientifique (CNRS), Aix-Marseille University (AMU), the Association Grégory Lemarchal and Vaincre la Mucoviscidose (project N° RF20190502466), and the Agence Nationale de la Recherche (LipInTB project N° ANR-19-CE44-0011). MS was supported by a PhD fellowship from the Association Grégory Lemarchal and Vaincre la Mucoviscidose (project n° RF20190502466). RA was supported by a PhD fellowship from the Agence Nationale de la Recherche (LipInTB project N° ANR-19-CE44-0011).

We thank Prof. Jean-Louis Herrmann (Université Versailles-Saint-Quentin-en-Yvelines, France) for sharing the *M. abscessus* S-LuxAB bacterial strain.

## **ABBREVIATIONS**

ABP, activity-based probe; au, arbitrary unit; AMK, amikacin; CC<sub>50</sub>, compound concentration leading to 50% of cell cytotoxicity; CF, cystic fibrosis; CFU, colony-forming units; ConA, Concanamycin A; CyC, Cyclosporins and Cyclophostin analogues; IMP, imipenem; INH, isoniazid; MIC<sub>50Raw</sub>, minimal compound concentration leading to a 50% decrease in CFU count as compared to untreated cells; MIC<sub>90</sub>, minimal inhibitory concentration leading to 90% of growth inhibition; NTM, nontuberculous mycobacterial; REMA, resazurin microtiter assay; RFU%, relative fluorescence units.

## REFERENCES

- (1) WHO, Global tuberculosis report. **2022**, <https://www.who.int/teams/global-tuberculosis-programme/data>.
- (2) Aubry, A.; Mougari, F.; Reibel, F.; Cambau, E., *Mycobacterium marinum*. *Microbiol Spectr* **2017**, *5* (2).
- (3) Stout, J. E.; Koh, W. J.; Yew, W. W., Update on pulmonary disease due to non-tuberculous mycobacteria. *Int J Infect Dis* **2016**, *45*, 123-134.
- (4) Swenson, C.; Zerbe, C. S.; Fennelly, K., Host Variability in NTM Disease: Implications for Research Needs. *Front Microbiol* **2018**, *9* (2901), 2901.
- (5) Tortoli, E.; Fedrizzi, T.; Meehan, C. J.; Trovato, A.; Grottola, A.; Giacobazzi, E.; Serpini, G. F.; Tagliazucchi, S.; Fabio, A.; Bettua, C.; Bertorelli, R.; Frascaro, F.; De Sanctis, V.; Pecorari, M.; Jousson, O.; Segata, N.; Cirillo, D. M., The new phylogeny of the genus *Mycobacterium*: The old and the news. *Infect Genet Evol* **2017**, *56*, 19-25.
- (6) van Ingen, J.; Wagner, D.; Gallagher, J.; Morimoto, K.; Lange, C.; Haworth, C. S.; Floto, R. A.; Adjemian, J.; Prevots, D. R.; Griffith, D. E.; Ntm, N. E. T., Poor adherence to management guidelines in nontuberculous mycobacterial pulmonary diseases. *Eur Respir J* **2017**, *49* (2), 1601855.
- (7) Schiff, H. F.; Jones, S.; Achaiah, A.; Pereira, A.; Stait, G.; Green, B., Clinical relevance of non-tuberculous mycobacteria isolated from respiratory specimens: seven year experience in a UK hospital. *Scientific Reports* **2019**, *9* (1), 1730.
- (8) Wetzstein, N.; Geil, A.; Kann, G.; Lehn, A.; Schuttfort, G.; Kessel, J.; Bingold, T. M.; Kupper-Tetzel, C. P.; Haberl, A.; Graf, C.; Vehreschild, M.; Stephan, C.; Hogardt, M.; Wichelhaus, T. A.; Wolf, T., Disseminated disease due to non-tuberculous mycobacteria in HIV positive patients: A retrospective case control study. *PLoS One* **2021**, *16* (7), e0254607.
- (9) Roux, A. L.; Catherinot, E.; Ripoll, F.; Soismier, N.; Macheras, E.; Ravilly, S.; Bellis, G.; Vibet, M. A.; Le Roux, E.; Lemonnier, L.; Gutierrez, C.; Vincent, V.; Fauroux, B.; Rottman, M.; Guillemot, D.; Gaillard, J. L.; Jean-Louis Herrmann for the, O. M. A. G., Multicenter study of prevalence of nontuberculous mycobacteria in patients with cystic fibrosis in france. *J Clin Microbiol* **2009**, *47* (12), 4124-4128.
- (10) Leung, J. M.; Olivier, K. N., Nontuberculous mycobacteria in patients with cystic fibrosis. *Semin Respir Crit Care Med* **2013**, *34* (1), 124-134.
- (11) Park, I. K.; Olivier, K. N., Nontuberculous mycobacteria in cystic fibrosis and non-cystic fibrosis bronchiectasis. *Semin Respir Crit Care Med* **2015**, *36* (2), 217-224.
- (12) Roux, A. L.; Viljoen, A.; Bah, A.; Simeone, R.; Bernut, A.; Laencina, L.; Deramaudt, T.; Rottman, M.; Gaillard, J. L.; Majlessi, L.; Brosch, R.; Girard-Misguich, F.; Vergne, I.; de Chastellier, C.; Kremer, L.; Herrmann, J. L., The distinct fate of smooth and rough *Mycobacterium abscessus* variants inside macrophages. *Open biology* **2016**, *6* (11), 160185.
- (13) Boudehen, Y. M.; Kremer, L., *Mycobacterium abscessus*. *Trends Microbiol* **2021**, *29* (10), 951-952.
- (14) Johansen, M. D.; Herrmann, J. L.; Kremer, L., Non-tuberculous mycobacteria and the rise of *Mycobacterium abscessus*. *Nat Rev Microbiol* **2020**, *18* (7), 392-407.

- (15) Catherinot, E.; Clarissou, J.; Etienne, G.; Ripoll, F.; Emile, J. F.; Daffe, M.; Perronne, C.; Soudais, C.; Gaillard, J. L.; Rottman, M., Hypervirulence of a rough variant of the *Mycobacterium abscessus* type strain. *Infect Immun* **2007**, *75* (2), 1055-1058.
- (16) Catherinot, E.; Roux, A. L.; Macheras, E.; Hubert, D.; Matmar, M.; Dannhoffer, L.; Chinet, T.; Morand, P.; Poyart, C.; Heym, B.; Rottman, M.; Gaillard, J. L.; Herrmann, J. L., Acute respiratory failure involving an R variant of *Mycobacterium abscessus*. *J Clin Microbiol* **2009**, *47* (1), 271-274.
- (17) Jönsson, B. E.; Gilljam, M.; Lindblad, A.; Ridell, M.; Wold, A. E.; Welinder-Olsson, C., Molecular epidemiology of *Mycobacterium abscessus*, with focus on cystic fibrosis. *J Clin Microbiol* **2007**, *45* (5), 1497-1504.
- (18) Surette, M. G., The cystic fibrosis lung microbiome. *Ann Am Thorac Soc* **2014**, *11 Suppl 1*, S61-5.
- (19) Kiedrowski, M. R.; Bomberger, J. M., Viral-Bacterial Co-infections in the Cystic Fibrosis Respiratory Tract. *Front Immunol* **2018**, *9* (3067), 3067.
- (20) Lim, A. Y. H.; Chotirmall, S. H.; Fok, E. T. K.; Verma, A.; De, P. P.; Goh, S. K.; Pua, S. H.; Goh, D. E. L.; Abisheganaden, J. A., Profiling non-tuberculous mycobacteria in an Asian setting: characteristics and clinical outcomes of hospitalized patients in Singapore. *BMC Pulm Med*. **2018**, *18* (1), 85-85.
- (21) Pierre-Audigier, C.; Ferroni, A.; Sermet-Gaudelus, I.; Le Bourgeois, M.; Offredo, C.; Vu-Thien, H.; Fauroux, B.; Mariani, P.; Munck, A.; Bingen, E.; Guillemot, D.; Quesne, G.; Vincent, V.; Berche, P.; Gaillard, J. L., Age-related prevalence and distribution of nontuberculous mycobacterial species among patients with cystic fibrosis. *J Clin Microbiol*. **2005**, *43* (7), 3467-3470.
- (22) Nessar, R.; Cambau, E.; Reyrat, J. M.; Murray, A.; Gicquel, B., *Mycobacterium abscessus*: a new antibiotic nightmare. *J Antimicrob Chemother*. **2012**, *67* (4), 810-818.
- (23) Osmani, M.; Sotello, D.; Alvarez, S.; Odell, J. A.; Thomas, M., *Mycobacterium abscessus* infections in lung transplant recipients: 15-year experience from a single institution. *Transpl Infect Dis* **2018**, *20* (2), e12835.
- (24) Cavalier, J. F.; Spilling, C. D.; Durand, T.; Camoin, L.; Canaan, S., Lipolytic enzymes inhibitors: A new way for antibacterial drugs discovery. *Eur J Med Chem*. **2021**, *209*, 112908.
- (25) Nguyen, P. C.; Delorme, V.; Bénarouche, A.; Martin, B. P.; Paudel, R.; Gnawali, G. R.; Madani, A.; Puppo, R.; Landry, V.; Kremer, L.; Brodin, P.; Spilling, C. D.; Cavalier, J.-F.; Canaan, S., Cyclopostins and Cyclophostin analogs as promising compounds in the fight against tuberculosis. *Scientific Reports* **2017**, *7* (1), 11751.
- (26) Nguyen, P. C.; Madani, A.; Santucci, P.; Martin, B. P.; Paudel, R. R.; Delattre, S.; Herrmann, J. L.; Spilling, C. D.; Kremer, L.; Canaan, S.; Cavalier, J. F., Cyclophostin and Cyclopostins analogues, new promising molecules to treat mycobacterial-related diseases. *Int J Antimicrob Agents* **2018**, *51* (4), 651-654.
- (27) Madani, A.; Ridenour, J. N.; Martin, B. P.; Paudel, R. R.; Abdul Basir, A.; Le Moigne, V.; Herrmann, J. L.; Audebert, S.; Camoin, L.; Kremer, L.; Spilling, C. D.; Canaan, S.; Cavalier, J. F., Cyclopostins and Cyclophostin Analogues as Multitarget Inhibitors That Impair Growth of *Mycobacterium abscessus*. *ACS Infect Dis* **2019**, *5* (9), 1597-1608.
- (28) Point, V.; Malla, R. K.; Diomande, S.; Martin, B. P.; Delorme, V.; Carriere, F.; Canaan, S.; Rath, N. P.; Spilling, C. D.; Cavalier, J. F., Synthesis and kinetic evaluation of cyclophostin and

cyclipostins phosphonate analogs as selective and potent inhibitors of microbial lipases. *J Med Chem* **2012**, *55* (22), 10204-10219.

(29) Point, V.; Malla, R. K.; Carriere, F.; Canaan, S.; Spilling, C. D.; Cavalier, J. F., Enantioselective inhibition of microbial lipolytic enzymes by nonracemic monocyclic enolphosphonate analogues of cyclophostin. *J Med Chem* **2013**, *56* (11), 4393-4401.

(30) Viljoen, A.; Richard, M.; Nguyen, P. C.; Fourquet, P.; Camoin, L.; Paudal, R. R.; Gnawali, G. R.; Spilling, C. D.; Cavalier, J. F.; Canaan, S.; Blaise, M.; Kremer, L., Cyclipostins and cyclophostin analogs inhibit the antigen 85C from *Mycobacterium tuberculosis* both in vitro and in vivo. *J Biol Chem* **2018**, *293* (8), 2755-2769.

(31) Spilling, C. D.; Martin, B. P.; Canaan, S.; Cavalier, J.-F. Fluorescent Labeled Inhibitors. US10047112B2, August 14, 2018, 2018.

(32) Susani-Etzerodt, H.; Schmidinger, H.; Riesenhuber, G.; Birner-Gruenberger, R.; Hermetter, A., A versatile library of activity-based probes for fluorescence detection and/or affinity isolation of lipolytic enzymes. *Chem Phys Lipids* **2006**, *144* (1), 60-68.

(33) Dutta, S.; Malla, R. K.; Bandyopadhyay, S.; Spilling, C. D.; Dupureur, C. M., Synthesis and kinetic analysis of some phosphonate analogs of cyclophostin as inhibitors of human acetylcholinesterase. *Bioorg Med Chem* **2010**, *18* (6), 2265-2274.

(34) Malla, R. K.; Bandyopadhyay, S.; Spilling, C. D.; Dutta, S.; Dupureur, C. M., The first total synthesis of (+/-)-cyclophostin and (+/-)-cyclipostin P: inhibitors of the serine hydrolases acetyl cholinesterase and hormone sensitive lipase. *Org Lett* **2011**, *13* (12), 3094-3097.

(35) Vasilieva, E.; Dutta, S.; Malla, R. K.; Martin, B. P.; Spilling, C. D.; Dupureur, C. M., Rat hormone sensitive lipase inhibition by cyclipostins and their analogs. *Bioorg Med Chem* **2015**, *23* (5), 944-952.

(36) Blanot, D.; Lee, J.; Girardin, S. E., Synthesis and biological evaluation of biotinyl hydrazone derivatives of muramyl peptides. *Chem Biol Drug Des* **2012**, *79* (1), 2-8.

(37) Huang, J.; Liu, M.; Ma, X.; Dong, Q.; Ye, B.; Wang, W.; Zeng, W., A highly selective turn-off fluorescent probe for Cu(ii) based on a dansyl derivative and its application in living cell imaging. *RSC Advances* **2014**, *4* (44), 22964-22970.

(38) Hanson, P. R.; Chegondi, R.; Nguyen, J.; Thomas, C. D.; Waetzig, J. D.; Whitehead, A., Total synthesis of dolabelide C: a phosphate-mediated approach. *J Org Chem* **2011**, *76* (11), 4358-4370.

(39) Sauer, R.; Turshatov, A.; Balushev, S.; Landfester, K., One-Pot Production of Fluorescent Surface-Labeled Polymeric Nanoparticles via Miniemulsion Polymerization with Bodipy Surfmers. *Macromolecules* **2012**, *45* (9), 3787-3796.

(40) Fletcher, D. I.; Ganellin, C. R.; Piergentili, A.; Dunn, P. M.; Jenkinson, D. H., Synthesis and pharmacological testing of polyaminoquinolines as blockers of the apamin-sensitive Ca<sup>2+</sup>-activated K<sup>+</sup> channel (SK(Ca)). *Bioorg Med Chem* **2007**, *15* (16), 5457-5479.

(41) Ing, H. R.; Manske, R. H. F., CCCXII.—A modification of the Gabriel synthesis of amines. *J. Chem. Soc.* **1926**, *129* (0), 2348-2351.

(42) Niwa, M.; Morikawa, M.-a.; Nabeta, T.; Higashi, N., Preparation of Anthryl Group-Tagged Helical Poly( $\gamma$ -benzyl l-glutamate) Self-Assembled Film on Gold Surface and Its Interaction with DNA. *Macromolecules* **2002**, *35* (7), 2769-2775.

- (43) O'Brien, J.; Wilson, I.; Orton, T.; Pognan, F., Investigation of the Alamar Blue (resazurin) fluorescent dye for the assessment of mammalian cell cytotoxicity. *Eur J Biochem* **2000**, *267* (17), 5421-5426.
- (44) Christophe, T.; Jackson, M.; Jeon, H. K.; Fenistein, D.; Contreras-Dominguez, M.; Kim, J.; Genovesio, A.; Carralot, J. P.; Ewann, F.; Kim, E. H.; Lee, S. Y.; Kang, S.; Seo, M. J.; Park, E. J.; Skovierova, H.; Pham, H.; Riccardi, G.; Nam, J. Y.; Marsollier, L.; Kempf, M.; Joly-Guillou, M. L.; Oh, T.; Shin, W. K.; No, Z.; Nehrbass, U.; Brosch, R.; Cole, S. T.; Brodin, P., High content screening identifies decaprenyl-phosphoribose 2' epimerase as a target for intracellular antimycobacterial inhibitors. *PLoS Pathog* **2009**, *5* (10), e1000645.
- (45) Le Moigne, V.; Blouquit-Laye, S.; Desquesnes, A.; Girard-Misguich, F.; Herrmann, J. L., Liposomal amikacin and *Mycobacterium abscessus*: intimate interactions inside eukaryotic cells. *J Antimicrob Chemother* **2022**, <https://doi.org/10.1093/jac/dkac348>.
- (46) Takano, K.; Shimada, D.; Kashiwagura, S.; Kamioka, Y.; Hariu, M.; Watanabe, Y.; Seki, M., Severe Pulmonary *Mycobacterium abscessus* Cases Due to Co-Infection with Other Microorganisms Well Treated by Clarithromycin and Sitafloxacin in Japan. *Int Med Case Rep J* **2021**, *14*, 465-470.
- (47) Wynn, T. A.; Chawla, A.; Pollard, J. W., Macrophage biology in development, homeostasis and disease. *Nature* **2013**, *496* (7446), 445-455.
- (48) Huss, M.; Ingenhorst, G.; Konig, S.; Gassel, M.; Drose, S.; Zeeck, A.; Altendorf, K.; Wiczorek, H., Concanamycin A, the specific inhibitor of V-ATPases, binds to the V(o) subunit c. *J Biol Chem* **2002**, *277* (43), 40544-40548.
- (49) Griffith, D. E., *Mycobacterium abscessus* and Antibiotic Resistance: Same As It Ever Was. *Clin Infect Dis* **2019**, *69* (10), 1687-1689.
- (50) Shaw, L. P.; Doyle, R. M.; Kavaliunaite, E.; Spencer, H.; Balloux, F.; Dixon, G.; Harris, K. A., Children With Cystic Fibrosis Are Infected With Multiple Subpopulations of *Mycobacterium abscessus* With Different Antimicrobial Resistance Profiles. *Clin Infect Dis* **2019**, *69* (10), 1678-1686.
- (51) Barelier, S.; Avellan, R.; Gnawali, G. R.; Fourquet, P.; Roig-Zamboni, V.; Poncin, I.; Point, V.; Bourne, Y.; Audebert, S.; Camoin, L.; Spilling, C. D.; Canaan, S.; Cavalier, J. F.; Sulzenbacher, G., Direct capture, inhibition and crystal structure of HsaD (Rv3569c) from *M. tuberculosis*. *FEBS J* **2022**, <https://doi.org/10.1111/febs.16645>.
- (52) Greenwood, D. J.; Dos Santos, M. S.; Huang, S.; Russell, M. R. G.; Collinson, L. M.; MacRae, J. I.; West, A.; Jiang, H.; Gutierrez, M. G., Subcellular antibiotic visualization reveals a dynamic drug reservoir in infected macrophages. *Science (New York, N.Y.)* **2019**, *364* (6447), 1279-1282.
- (53) Santucci, P.; Greenwood, D. J.; Fearn, A.; Chen, K.; Jiang, H.; Gutierrez, M. G., Intracellular localisation of *Mycobacterium tuberculosis* affects efficacy of the antibiotic pyrazinamide. *Nat Commun* **2021**, *12* (1), 3816.
- (54) Schump, M. D.; Fox, D. M.; Bertozzi, C. R.; Riley, L. W., Subcellular Partitioning and Intramacrophage Selectivity of Antimicrobial Compounds against *Mycobacterium tuberculosis*. *Antimicrob Agents Chemother.* **2017**, *61* (3).
- (55) Sambandamurthy, V. K.; Derrick, S. C.; Hsu, T.; Chen, B.; Larsen, M. H.; Jalapathy, K. V.; Chen, M.; Kim, J.; Porcelli, S. A.; Chan, J.; Morris, S. L.; Jacobs, W. R., Jr., *Mycobacterium tuberculosis* DeltaRD1 DeltapanCD: a safe and limited replicating mutant strain that protects

immunocompetent and immunocompromised mice against experimental tuberculosis. *Vaccine* **2006**, *24* (37-39), 6309-6320.

(56) Bernut, A.; Herrmann, J. L.; Kissa, K.; Dubremetz, J. F.; Gaillard, J. L.; Lutfalla, G.; Kremer, L., *Mycobacterium abscessus* cording prevents phagocytosis and promotes abscess formation. *Proc Natl Acad Sci U S A* **2014**, *111* (10), E943-52.

(57) Palomino, J. C.; Martin, A.; Camacho, M.; Guerra, H.; Swings, J.; Portaels, F., Resazurin microtiter assay plate: simple and inexpensive method for detection of drug resistance in *Mycobacterium tuberculosis*. *Antimicrob Agents Chemother.* **2002**, *46* (8), 2720-2722.

(58) Rybniker, J.; Vocat, A.; Sala, C.; Busso, P.; Pojer, F.; Benjak, A.; Cole, S. T., Lansoprazole is an antituberculous prodrug targeting cytochrome bc1. *Nat Commun.* **2015**, *6*, 7659.

(59) Wiegand, I.; Hilpert, K.; Hancock, R. E., Agar and broth dilution methods to determine the minimal inhibitory concentration (MIC) of antimicrobial substances. *Nat Protoc* **2008**, *3* (2), 163-175.

(60) Santucci, P.; Dedaki, C.; Athanasoulis, A.; Gallorini, L.; Munoz, A.; Canaan, S.; Cavalier, J.-F.; Magrioti, V., Synthesis of long chain  $\beta$ -lactones and their antibacterial activities against pathogenic mycobacteria. *ChemMedChem* **2019**, *14* (3), 349-358.

(61) Dupont, C.; Viljoen, A.; Dubar, F.; Blaise, M.; Bernut, A.; Pawlik, A.; Bouchier, C.; Brosch, R.; Guerardel, Y.; Lelievre, J.; Ballell, L.; Herrmann, J. L.; Biot, C.; Kremer, L., A new piperidinol derivative targeting mycolic acid transport in *Mycobacterium abscessus*. *Mol Microbiol* **2016**, *101* (3), 515-529.

(62) Waskom, M., seaborn: statistical data visualization. *Journal of Open Source Software* **2021**, *6* (60), 3021.

(63) Postma, M.; Goedhart, J., PlotsOfData—A web app for visualizing data together with their summaries. *PLOS Biology* **2019**, *17* (3), e3000202.

**Table 1.** Antibacterial activities of the selected **CyC** compounds against various bacterial strains <sup>a</sup>

Cpds	MIC <sub>90</sub> (μM)								
	<i>M. smegmatis</i> mc <sup>2</sup> 155	<i>M. marinum</i> ATCC BAA-535/M	<i>M. bovis</i> BCG	<i>M. tuberculosis</i> mc <sup>2</sup> 6230	<i>M. abscessus</i> CIP 104536 <sup>T</sup>		<i>E. coli</i> DH10B	<i>P. aeruginosa</i> PAO1	<i>S. aureus</i>
					S variant	R variant			
AMK	-	2.9±0.17	0.82 ±0.05	0.63±0.03	5.8±0.20	10.1±0.45	-	-	-
INH	29.8±1.0	67.6 ±3.5	1.7±0.07	1.5±0.07	>100	>100	-	-	-
<b>CyC</b> <sub>17</sub> <sup>b</sup>	1.6±0.02	1.7±0.05	0.80±0.03	2.6±0.13	14.4±0.73	0.41±0.01	←	No effect	→
<b>CyC</b> <sub>31</sub>	35.1±0.46	16.5±2.3	0.87±0.06	5.3±0.15	1.2±0.30	27.1±1.6	←	No effect	→
<b>CyC</b> <sub>31</sub> -Dansyl	32.1±1.7	25.1±1.3	5.8±0.31	10.0±0.59	6.1±0.40	63.4±2.9	←	No effect	→
<b>CyC</b> <sub>32</sub>	55.5±1.6	37.0±0.56	1.1±0.15	5.4±0.70	168±2.0	>200	←	No effect	→
<b>CyC</b> <sub>32</sub> -Dansyl	55.7±2.4	37.3±0.90	7.4±0.89	13.3±0.57	>200	>200	←	No effect	→
<b>CyC</b> <sub>7α</sub> <sup>b</sup>	119±7.2	31.5±0.77	69.3±2.5	>200	>200	154±3.9	←	No effect	→
<b>CyC</b> <sub>7α</sub> -Dansyl	>200	44.4±2.0	62.3±1.8	>200	>200	>200	←	No effect	→
<b>CyC</b> <sub>7β</sub> <sup>b</sup>	164±3.4	6.0±0.40	47.2±2.0	37.2±3.9	>200	142±2.0	←	No effect	→
<b>CyC</b> <sub>7β</sub> -Dansyl	>200	19.5±1.2	32.0±1.1	60.5±3.0	>200	>200	←	No effect	→

<sup>a</sup> MIC<sub>90</sub>: compound minimal concentration leading to 90% of bacterial growth inhibition as determined by the REMA assay. Values are mean ± SD of two independent assays performed in triplicate. <sup>b</sup> Data for **CyC**<sub>17</sub> and **CyC**<sub>7(α,β)</sub> are from<sup>25-27</sup>. AMK, amikacin. INH, isoniazid.

**Table 2.** Antibacterial activities of the new **CyC** analogs against *M. abscessus* S infected macrophages

Cpds	CC <sub>50</sub> (μM) <sup>a</sup>	MIC <sub>50Raw</sub> (μM) <sup>b</sup>
IMP <sup>c</sup>	ND	28.3±4.7
CyC <sub>7α</sub> <sup>c</sup>	>100	29.3±2.9
CyC <sub>7β</sub> <sup>c</sup>	>70	65.3±6.2
CyC <sub>7α</sub> -Dansyl	>100	39.9±6.2
CyC <sub>7β</sub> -Dansyl	>100	80.6±7.1
CyC <sub>31</sub> (X=O)	>100	No effect
CyC <sub>32</sub> (X=CH <sub>2</sub> )	>100	No effect
CyC <sub>31</sub> -Dansyl (X=O)	>100	No effect
CyC <sub>32</sub> -Dansyl (X=CH <sub>2</sub> )	>100	No effect

<sup>a</sup> CC<sub>50</sub>: compound concentration leading to 50% Raw264.7 macrophages toxicity. <sup>b</sup> MIC<sub>50Raw</sub>: minimal compound concentration leading to a 50% decrease in CFU count as compared to untreated cells. Raw264.7 macrophages were infected by *M. abscessus* S-LuxAB at a MOI of 10, and further treated with each **CyC** or IMP for 24 h. The viable mycobacteria were quantified by measurement of luminescence which was further correlated to CFU. Untreated infected macrophages were used as control representing 100% of bacterial viability. MIC<sub>50Raw</sub> were calculated from curve fitting of CFU% as a function of the inhibitor concentration and are expressed as mean values of three independent assays. <sup>c</sup> Data from<sup>27</sup>. IMP, imipenem. ND: not determined.

## FIGURE LEGENDS

**Figure 1.** (A) Chemical structure of Cyclophostins & Cyclophostin analogs (CyC),<sup>25, 27</sup> with (B) the best CyC growth inhibitors. MIC<sub>90</sub>, compound concentration leading to 90% bacterial growth inhibition in culture medium; MIC<sub>50Raw</sub>, compound concentration leading to a 50% decrease in CFU count in infected Raw264.7 macrophages as compared to untreated cells. Log P values were computed using the ALOGPS 2.1 applet (<http://www.vcclab.org>). (C) Chemical structure of fluorescent CyC affinity probes.

**Figure 2.** Synthesis of the Dansyl-labeled (A) enolphosphonate CyC<sub>7(a,β)</sub>-Dansyl; (B) phosphate CyC<sub>31</sub>-Dansyl and phosphonate CyC<sub>32</sub>-Dansyl analogs of Cyclophostins; as well as (C) the corresponding CyC<sub>31</sub> and CyC<sub>32</sub> unlabeled compounds. The 11-bromo-1-undecanamine **20** was prepared according to literature procedure.<sup>39</sup> Log P values were computed using the ALOGPS 2.1 applet (<http://www.vcclab.org>).

**Figure 3. The CyC-Dansyl probes are able to label all mycobacterial strains regardless of their antibacterial activity.** (A) Representative fluorescence images of *M. smegmatis*, *M. abscessus* S and R, *M. marinum*, *M. bovis* BCG and *M. tuberculosis* mc<sup>2</sup>6230 strains in presence of fluorescent CyC. The mycobacteria were exposed to 200 μM CyC-Dansyl for 3 h, washed and fixed with 4% paraformaldehyde. Fixed bacteria were imaged using an Olympus IX81 confocal microscope. Scale bars: 2 μm. (B) Total fluorescence intensity of each CyC-Dansyl-treated mycobacteria expressed as arbitrary units (au) recorded at  $\lambda_{ex}/\lambda_{em} = 400/535 \pm 10$  nm using a Tecan Spark 10M multimode microplate reader (Tecan Group Ltd, France). Compounds color code is indicated in panel (A). Statistical significance was assessed with one-way ANOVA followed by Tukey post-hoc test using Prism 4.0 (Graphpad, Inc): \*\*  $p$ -value<0.01; \*\*\*  $p$ -value<0.001; *ns*, not significant ( $p$ -value>0.05). Results are corresponding to  $n=3$  biologically independent experiments performed in triplicate. (C) Cellular localization of the CyC<sub>31</sub>-Dansyl in *M. abscessus* S. The bacteria were exposed to 200 μM CyC<sub>31</sub>-Dansyl for 3 h, then washed and lysed. Equal amounts of proteins (50 μg) from total lysate (a), insoluble (b) and soluble (c) fractions recovered after centrifugation were separated by 12% SDS-PAGE and visualized by Coomassie blue staining (left) or in-gel fluorescence (right). The CyC<sub>31</sub>-Dansyl-labeled proteins were detected by fluorescent gel scanning using trans-UV illumination ( $\lambda_{ex}$  302 nm) as excitation source, and as emission the 530/28 filter of a ChemiDoc MP Imager (Bio-Rad) before staining of the gels with Coomassie Brilliant Blue dye. (D) 3-D reconstruction of a stack of deconvoluted images of CyC<sub>31</sub>-Dansyl-treated *M. abscessus* S cells from an epi-fluorescence microscope. XY (left panel) and YZ (right panel) orthogonal views. The bacterium was incubated with CyC<sub>31</sub>-Dansyl (green fluorescence) and the bacterial membrane was further stained with Nile Red (red fluorescence). The orange color

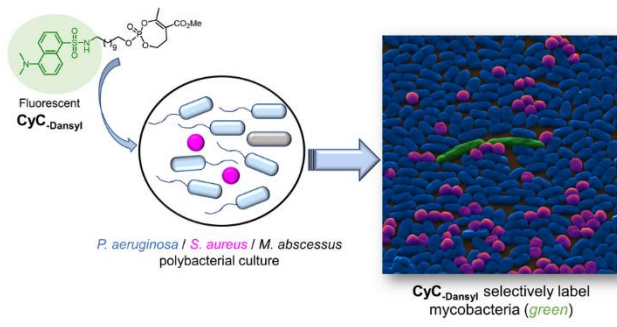
results from merge fluorescence between the Dansyl and the Nile Red (See also **Movie S1**). Scale bars: 0.5  $\mu\text{m}$ . **(E)** The  $\text{CyC}_{\text{-Dansyl}}$  probes specifically label *M. abscessus* cells in polybacterial cultures. Fluorescence micrographs of polybacterial cultures formed by *M. abscessus*-tdTomato, *P. aeruginosa* and *S. aureus* stained by  $\text{CyC}_{31\text{-Dansyl}}$  after overnight culture in 7H9 media for mycobacterial enrichment. Scale bars: 20  $\mu\text{m}$ .

**Figure 4. The  $\text{CyC}_{31\text{-Dansyl}}$  and  $\text{CyC}_{7\alpha\text{-Dansyl}}$  specifically localized on *M. abscessus* S inside infected Raw264.7 macrophages.** Representative images of the  $\text{CyC}_{31\text{-Dansyl}}$  and  $\text{CyC}_{7\alpha\text{-Dansyl}}$  distribution in intracellular *M. abscessus* S-dtTomato strains. **(A, C)** Raw264.7 macrophages were preincubated with 100  $\mu\text{M}$   $\text{CyC}_{31\text{-Dansyl}}$  **(A)** or  $\text{CyC}_{7\alpha\text{-Dansyl}}$  **(C)** for 24 h prior to be infected with *M. abscessus* S-dtTomato (MOI 10) for another 24 h. **(B, D)** Alternatively, *M. abscessus* S-dtTomato infected Raw264.7 were treated with each inhibitor for 24 h before chemical fixation and confocal fluorescence imaging. Scale bars: 5  $\mu\text{m}$ . Micrographs are representative of 2 independent experiments. **(E)** Quantitative analysis of the Dansyl fluorescence signal per bacterium and Raw264.7 cell positive area shown as a sinaplot-boxplot and expressed as arbitrary units (au). Results are from two biologically independent experiments; 122 to 258 cells were observed resulting in 389 to 808 segmented intracellular *M. abscessus* S-dtTomato positive regions. The *p*-values were calculated by using a two-tailed *t*-statistic test with Prism 4.0 (Graphpad, Inc): \*\*\* *p*-value<0.001. **(F-G)** Density plot of the Dansyl-fluorescent signal profile of *M. abscessus* S-dtTomato and Raw264.7 positive cells.

**Figure 5.  $\text{CyC}_{7(\alpha,\beta)\text{-Dansyl}}$  accumulate in acidic compartments inside Raw264.7 macrophages.** Raw264.7 macrophages were preincubated with 100  $\mu\text{M}$   $\text{CyC}_{7\alpha\text{-Dansyl}}$  **(A)** or  $\text{CyC}_{7\beta\text{-Dansyl}}$  **(B)** for 24 h in presence or absence of 100 nM Concanamycin A (ConA) prior to be stained with 1X BioTracker™ NIR633 dye and processed for confocal fluorescence imaging. Micrographs are representative of 106 to 136 observed cells from two biologically independent experiments. Scale bars: 5  $\mu\text{m}$ . **(C)** Disruption of endolysosomal acidification impairs  $\text{CyC}_{\text{-Dansyl}}$  colocalization with *M. abscessus* cells inside infected Raw264.7 macrophages. *M. abscessus* S-dtTomato infected Raw264.7 macrophages treated with 100 nM Concanamycin A (ConA) were preincubated with 100  $\mu\text{M}$   $\text{CyC}_{7\alpha\text{-Dansyl}}$  or  $\text{CyC}_{7\beta\text{-Dansyl}}$  for 24 h prior to be stained with 1X BioTracker™ NIR633 dye and processed for confocal fluorescence imaging. Micrographs are representative of around 120 observed cells from two biologically independent experiments. Scale bars: 5  $\mu\text{m}$  **(D)** Addition of ConA suppresses the intracellular antibacterial activity of  $\text{CyC}_{7\alpha}$  and  $\text{CyC}_{7\beta}$  against *M. abscessus* in infected Raw264.7 murine macrophages. Cells were infected at a multiplicity of infection (MOI) of 10 with *M. abscessus* S-LuxAB and treated for 24 h with 50  $\mu\text{M}$   $\text{CyC}_{7\alpha}$  /  $\text{CyC}_{7\beta}$ , or 267  $\mu\text{M}$  imipenem (IMP) as positive drug control, in presence or absence of 100 nM ConA. Surviving bacteria were next quantified from macrophage lysates by measurement of

luminescence, which was further correlated to CFU. Untreated infected macrophages in presence (*i.e.*,  $0.97 \pm 0.21 \times 10^6$  CFU) or absence (*i.e.*,  $1.04 \pm 0.11 \times 10^6$  CFU) of ConA were used as control representing 100% of bacterial viability. Results are shown as mean  $\pm$  standard error of the mean of three independent assays. The *p*-values were calculated by using a two-tailed *t*-statistic test with Prism 4.0 (Graphpad, Inc): \*\*\*, *p*-value<0.001. \*\*, *p*-value<0.01. *ns*, not significant (*p*-value>0.05). **(E)** The antibacterial activity of the CyC against extracellular *M. abscessus* S growth is not pH-dependent. Activity of **CyC<sub>7 $\alpha$</sub>** , **CyC<sub>7 $\beta$</sub>**  and **CyC<sub>31</sub>** against *M. abscessus* S replicating in broth medium, expressed as normalized relative fluorescence units (RFU%). *M. abscessus* S strains were grown until reaching mid-exponentially growing phase in 7H9-S medium, inoculated in fresh media adjusted at pH 7.0, 6.5, 6.0 or 5.5, and further used in susceptibility testing using the REMA assay towards the three **CyC** compounds. Each value is the mean  $\pm$  SD of two independent assays.

## For Table of Contents Only



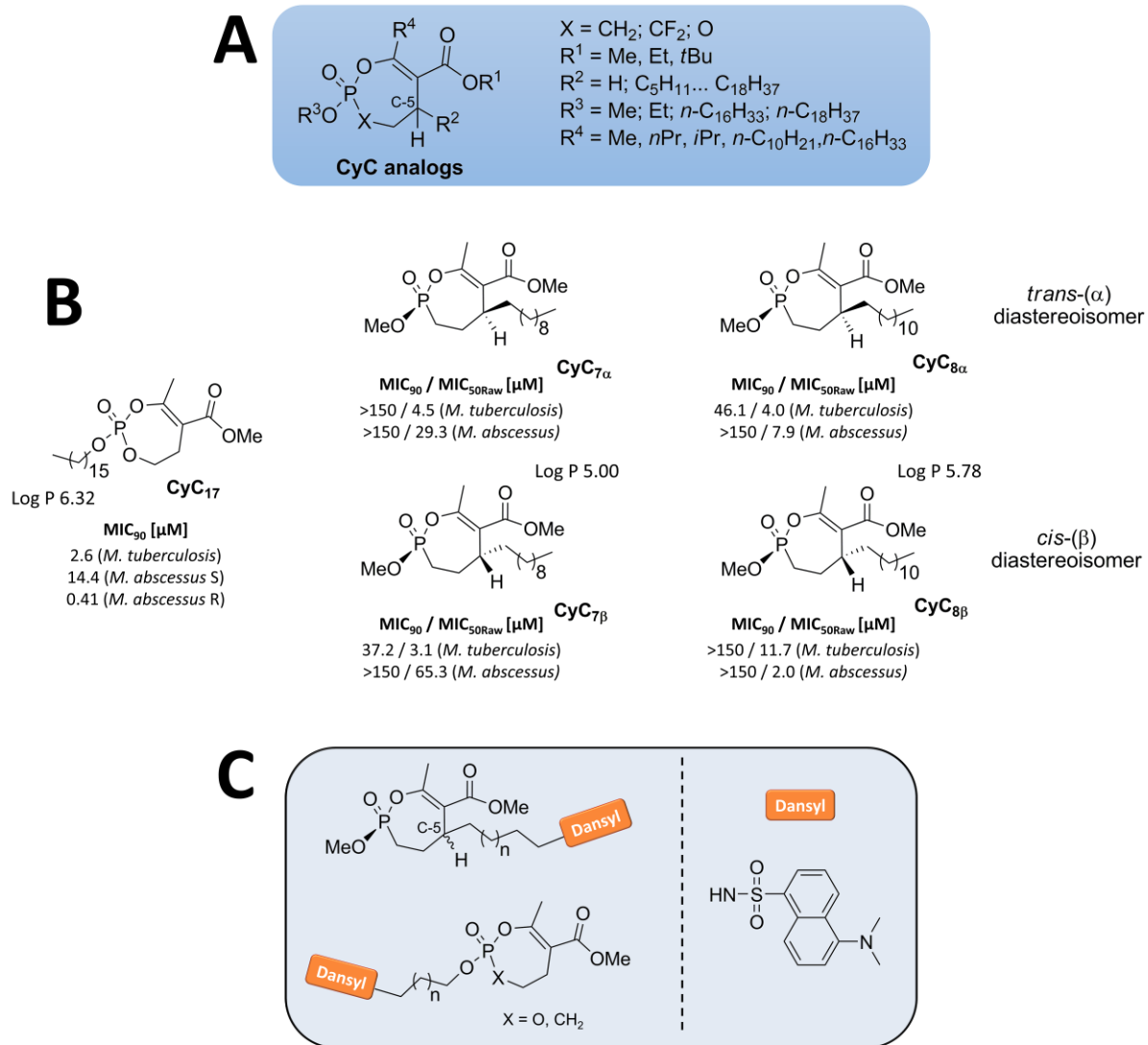


Figure 1

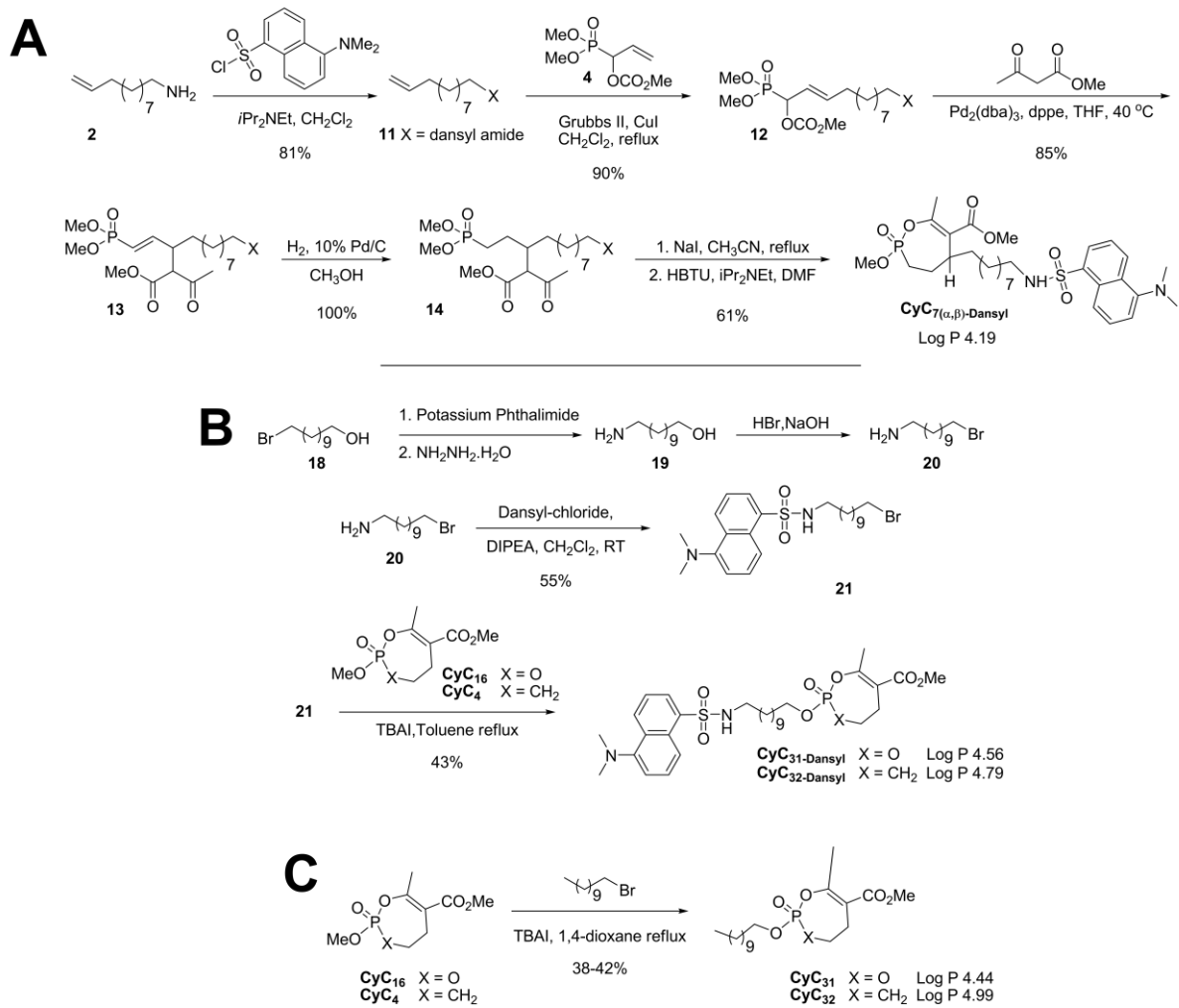


Figure 2

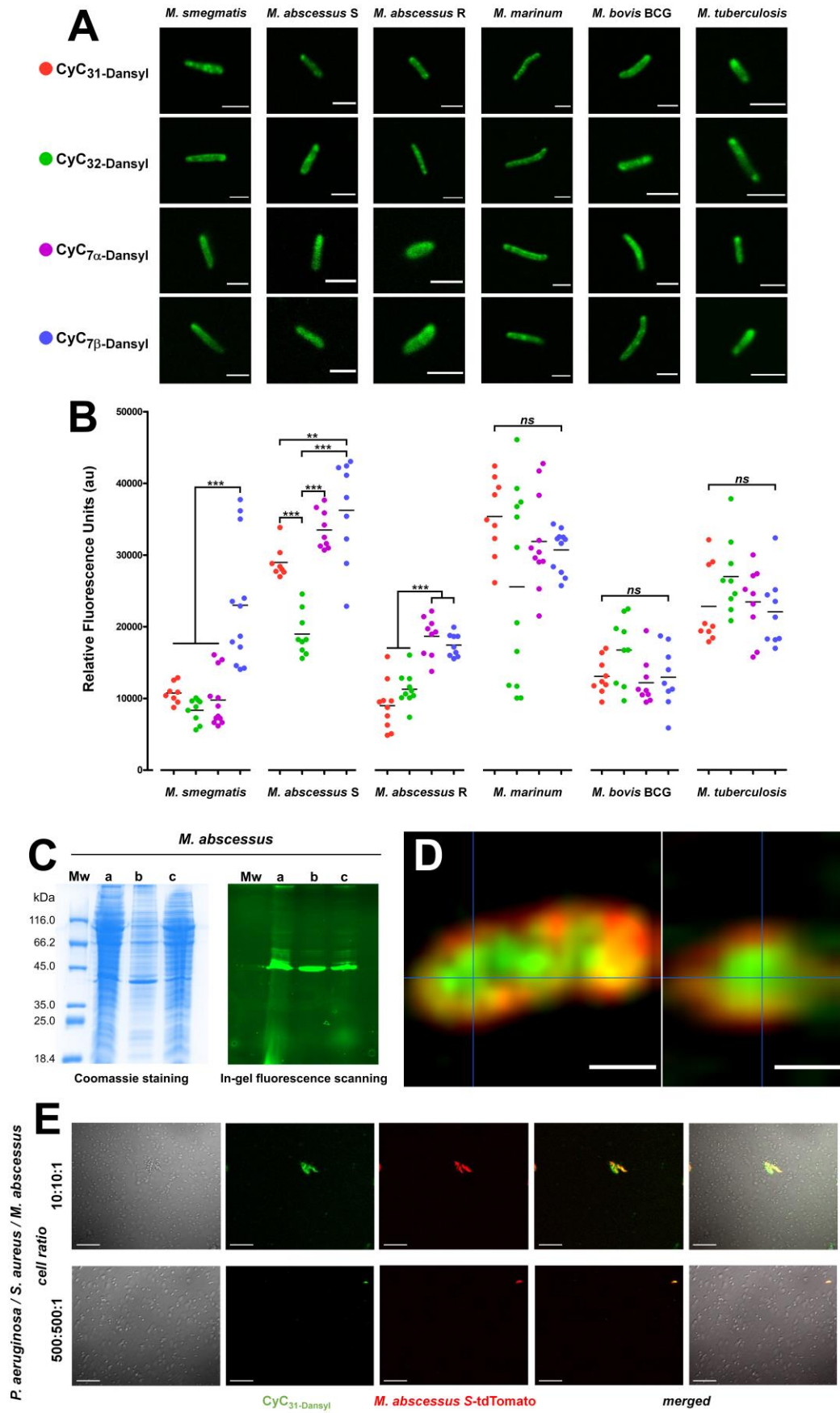


Figure 3

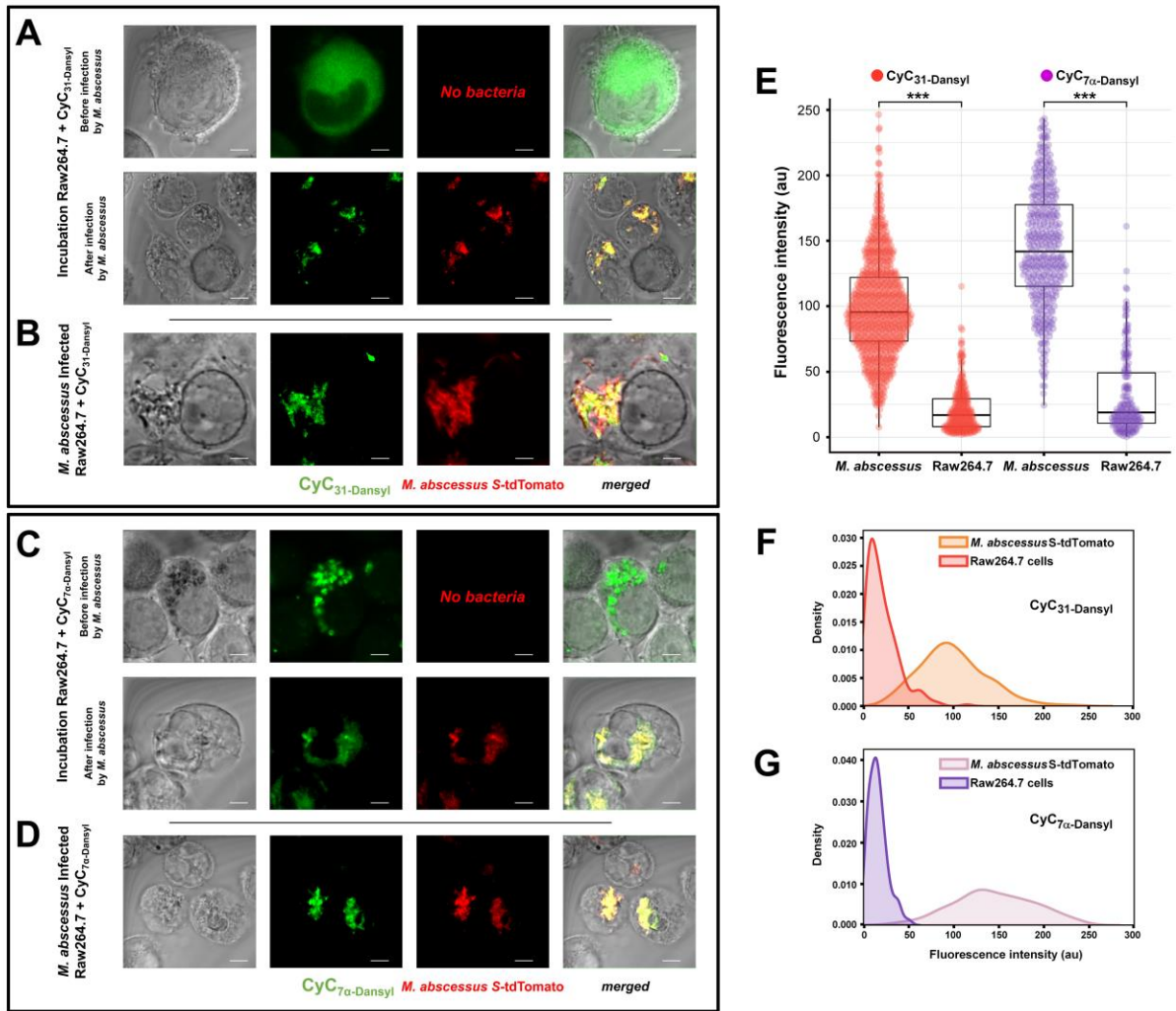


Figure 4

